ORNL/TM-10606

ornl

OAK RIDGE NATIONAL LABORATORY

MARTIN MARIETTA

An Investigation of Ceramic Coatings for Protection of SiC from High-Temperature Corrosion

J. I. Federer

OPERATED BY
MARTIN MARIETTA ENERGY SYSTEMS, INC.
FOR THE UNITED STATES
DEPARTMENT OF ENERGY

Printed in the United States of America. Available from
National Technical Information Service
U.S. Department of Commerce
5285 Port Royal Road, Springfield, Virginia 22161
NTIS price codes—Printed Copy: A04 Microfiche A01

ORNL/TM-10606

Metals and Ceramics Division

AN INVESTIGATION OF CERAMIC COATINGS FOR PROTECTION OF SiC FROM HIGH-TEMPERATURE CORROSION

J. I. Federer

Date Published - February 1988

NOTICE: This document contains information of a preliminary nature. It is subject to revision or correction and therefore does not represent a final report.

Prepared for the
Office of Industrial Programs
ED 01 01 00 0

Prepared by
OAK RIDGE NATIONAL LABORATORY
Oak Ridge, Tennessee 37831
MARTIN MARIETTA ENERGY SYSTEMS, INC.
for the
U.S. DEPARTMENT OF ENERGY
under contract DE-AC05-84OR21400

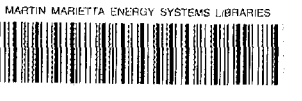

CONTENTS

LIST OF FIGURES

LIST OF TABLES

AN INVESTIGATION OF CERAMIC COATINGS FOR PROTECTION OF SiC FROM HIGH-TEMPERATURE CORROSION*

J. I. Federer

ABSTRACT

Silicon carbide (SiC) ceramics are susceptible to corrosion by certain industrial furnace environments. This behavior would limit the use of SiC components in ceramic heat exchangers. Because oxide ceramics corrode substantially less in the same environments, ceramic coatings have been investigated for corrosion protection. Coatings with Al_2O_3, SiO_2, or ZrO_2 as the main constituent were applied to sintered alpha and recrystallized (CS101) SiC substrates. The coated specimens were thermally cycled between room temperature and 1200°C as a test of adherence. Some coatings adhered better to the inherently rougher CS101 SiC; however, most coatings did not adhere to either substrate. Two Al_2O_3-based coatings developed cracks but remained intact during thermal cycling, and two ZrO_2-based coatings were adherent without cracks. These four coatings were subjected to corrosion testing at 1200°C in an oxidizing atmosphere containing Na_2CO_3. None of these four coatings exhibited the desired corrosion resistance in this test. Coated samples, however, corroded less than an uncoated sample, indicating that coatings can improve corrosion resistance.

---

1. INTRODUCTION

Silicon carbide (SiC) ceramics possess properties that are attractive for high-temperature heat exchanger applications. These properties include high strength and thermal conductivity and excellent resistance to thermal shock and oxidation. As a result, these materials have been selected as candidates for tubes and other components in various ceramic recuperators intended to recover heat from industrial furnace flue gases.[1-7] Corrosion resistance of materials is a primary concern in these applications. Although some industrial furnace atmospheres are relatively

---

*Research sponsored by the Waste Energy Recovery Program, Office of Industrial Programs, U.S. Department of Energy, under contract DE-AC05-84OR21400 with Martin Marietta Energy Systems, Inc.

clean, others contain combustion products or product carryover that corrode and/or foul heat exchanger elements. For example, the combustion products of natural gas contain mainly N_2, CO_2, H_2O, and excess O_2, whereas the combustion products of some No. 6 residual oil[5] contain these constituents, various metal oxides, and possibly other compounds. The flue gases of aluminum remelt furnaces sometimes contain alkali halides as a result of fluxing operations, and the flue gases of glass furnaces and steel soaking pits often carry a heavy burden of particulates.

Although SiC ceramics are resistant to high-temperature oxidation, these materials are susceptible to corrosion by certain industrial furnace environments. For example, severe corrosion has occurred in aluminum remelt[8-10] and glass furnace atmospheres.[11] Recession rates as high as 3 mm/year have been measured in an aluminum remelt furnace.[8] Laboratory tests have shown that corrosion is caused by alkali compounds[12-15] (which are contained in many industrial furnace atmospheres) at planned use temperatures of ceramic recuperators, ~1000 to ~1200°C. Corrosion by NaCl, NaF, Na_2SO_4, and Na_2CO_3 causes surface recession beneath a silicate reaction product.

Corrosion increases the construction and operating costs of heat exchangers. Thicker cross sections must be used in vulnerable components, or the components must be replaced more frequently. A buildup of corrosion products might affect heat transfer and reduce heat exchanger efficiency. Alternatively, heat exchangers could be operated at a low enough temperature that corrosion would be less severe; however, this approach also lowers efficiency and defeats the purpose of using a ceramic recuperator. A possible remedy to the corrosion problem is a protective coating on the SiC. In several tests wherein SiC corroded severely, oxide ceramics corroded substantially less.[9,10] High-alumina ceramics were particularly resistant to corrosion. In recognition of this fact, a survey of commercially available ceramic coatings was made.[17] The coatings included in the compilation had Al_2O_3, Cr_2O_3, SiO_2, TiO_2, and ZrO_2 as the main constituents; however, the ability of any of these coatings to protect SiC from corrosion was unknown.

In the current study, some of the ceramic coatings identified in the survey were evaluated as candidates for protecting SiC from corrosion. The study involved coatings of various compositions, different application methods, thermal cycling to determine adherence, and corrosion testing in a laboratory furnace. The objective was to identify one or more coatings that protect SiC sufficiently well in laboratory tests to qualify for testing in industrial furnace atmospheres.

2. CORROSION OF SiC BY ALKALI COMPOUNDS

Silicon carbide resists oxidation in air at temperatures up to at least 1400°C. Resistance is provided by a thin, adherent, self-healing layer of SiO_2 that minimizes access of O_2 to the SiC. Pure SiO_2 melts at 1710°C; sodium monoxide (Na_2O), however, greatly decreases the melting point. A eutectic melting below 800°C occurs at ~25 wt % Na_2O. A mixture of liquid and crystalline phases (quartz, tridymite, and cristobalite) exists between pure SiO_2 and the eutectic composition over the temperature range 800 to 1710°C. Thus, deposition of Na_2O in the SiO_2 layer decreases the refractoriness of the normally protective layer. The chemically altered layer apparently does not prevent access of O_2 to the SiC, which then oxidizes.

Several compounds have been shown to cause corrosion of SiC in oxidizing atmospheres: NaCl, NaF, Na_2SO_4, and Na_2CO_3. Analagous compounds of potassium would probably cause similar corrosion. Possible steps in the corrosion process (using Na_2CO_3 as the corrodent) are as follows:

1. Reaction between Na_2CO_3 and the normally protective SiO_2 layer at 1000 to 1200°C to form a compound and gas,

$$Na_2CO_3(v) + xSiO_2(s) \rightarrow Na_2O{\cdot}xSiO_2(l) + CO_2(g),$$
$$\text{where } x = 0.5,\ 1,\ \text{or } 2.$$

2. $Na_2O{\cdot}xSiO_2$, being liquid, equilibrates with the remaining SiO_2 to form a mixture of liquid and crystalline SiO_2 phases.
3. O_2 diffuses through the chemically altered SiO_2 layer to the SiC, which oxidizes to SiO_2 and CO_2,

$$SiC(s) + 2O_2(g) \rightarrow SiO_2(s,l) + CO_2(g) .$$

A characteristic feature of SiC corroded by alkali compounds is the presence of a previously molten silicate glass layer containing alkali oxides and gas bubbles.

3. POTENTIAL CORROSION PROTECTION BY CERAMIC COATINGS

Coatings can protect materials from corrosion by at least two methods. First, a coating could form an impenetrable layer to corrodents; unfortunately, no such coating for SiC is known. Second, a coating could lessen the effect of reaction by becoming part of the corrosion product. By introducing one or more refractory compounds into the corrosion product, the refractoriness of the SiO_2-rich layer might be increased. For example, all compositions in the Na_2O-SiO_2 binary system are partially or totally liquid at temperatures above ~1000°C, whereas certain compositions in the Na_2O-SiO_2-Al_2O_3 ternary system are solids at the same temperature. A coating containing a high Al_2O_3 content, therefore, might equilibrate beneficially with the chemically altered SiO_2 layer. Similarly, other refractory compounds such as MgO, TiO_2, and ZrO_2 might also assist in maintaining higher refractoriness in the reaction product. A potential problem with this approach is the wide range of compositions wherein liquids form in complex systems. Nonuniformity of composition might also cause localized melting, even though the average composition would be solid. In addition, the diffusion rate of oxygen in a solid coating might be faster than in the normally protective SiO_2 layer.

4. SUBSTRATE MATERIALS

Initially, sintered alpha SiC (SA)* was the only substrate material used. As typically fabricated, this material contains ~99 wt % SiC and has a density of 3.1 g/cm^3 (97% of theoretical density). The material was obtained as tubing in two sizes: 25-mm OD by 19-mm ID and 19-mm OD by 16-mm ID. The mean surface roughness of several randomly selected specimens of each type was ~1 μm (~40 μin.). Because many coatings do not adhere to SA, recrystallized SiC (CS101)† in the form of 16-mm-diam

*Standard Oil Engineered Materials Co., Niagara Falls, NY.

†Norton Company, Worcester, MA.

rods was used later in the work. CS101 also contains ~99 wt % SiC, but it has a rougher surface because of a porosity of ~15 vol %. The mean surface roughness of several specimens of CS101 was 13 μm (500 μin.). Characteristics of the SiC substrates are summarized in Table 1, wherein the two sizes of SA tubes are designated SA-1 and SA-2.

Table 1. Characteristics of SiC substrates

	Material		
	SA-1	SA-2	CS101
SiC content, wt %	~99	~99	~99
Density, g/cm^3	3.1	3.1	2.7
Surface roughness, μm	1	1	13
Dimensions, mm			
OD	25	19	16
ID	19	16	
Length	100	100	75

Polished cross sections of the substrate materials (Fig. 1) show that SA was much smoother than CS101. The latter material was tried as a substrate to take advantage of possible mechanical bonding to the rougher surface associated with the surface-connected porosity.

Specimens of SA-1 and SA-2 measuring 100 mm long and of CS101 measuring 75 mm long were cut from the original stock with a diamond abrasive saw. A notch measuring ~2 mm wide by ~1 mm deep was cut into one end of each specimen. With the notch as a reference mark, four diameter measurements were made at each end and in the middle at the 1-5, 2-6, 3-7, and 4-8 positions shown in Fig. 2, so that coating thicknesses could be determined. Surface roughness measurements were made in the same locations on some specimens.

Substrates of SA material were sent from Oak Ridge National Laboratory (ORNL) to several commercial vendors for coating. Because of vendor efforts to prepare the surfaces for coating and the possible mixing of the identity of the specimens, coating thicknesses determined by micrometer measurements were considered to be only approximate values. Coating thicknesses were accurately determined by optical measurements on polished cross sections of some specimens.

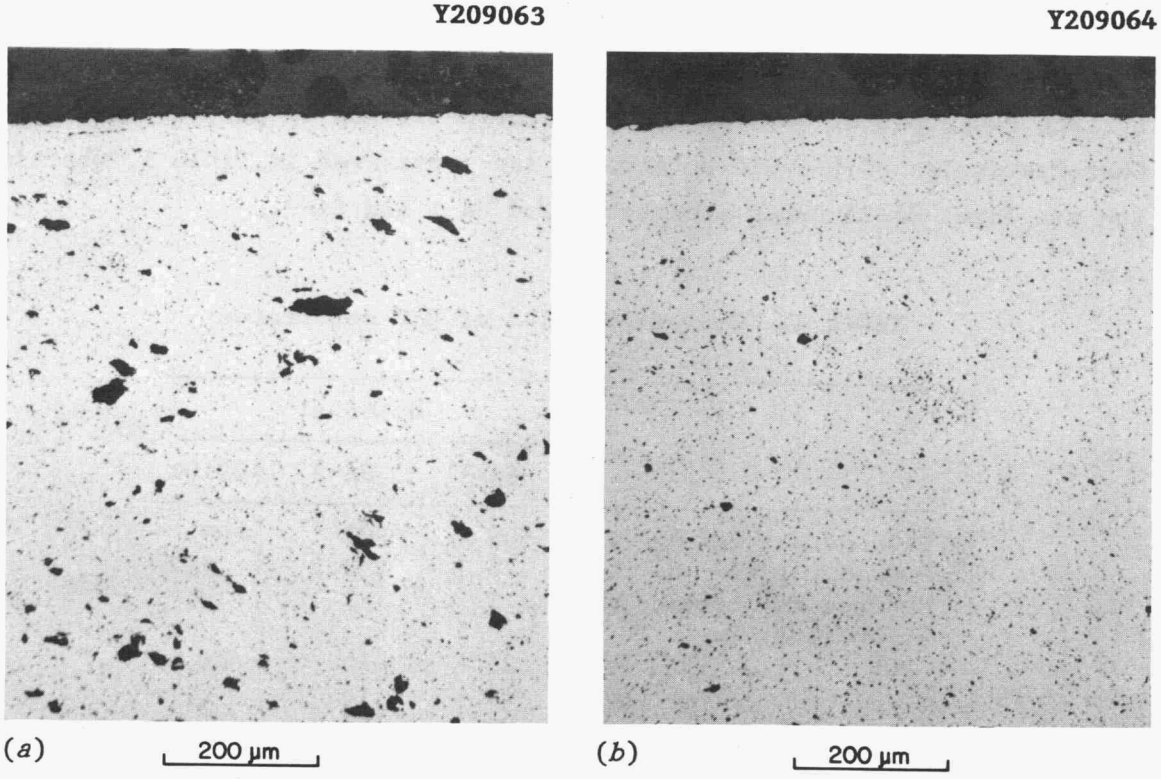

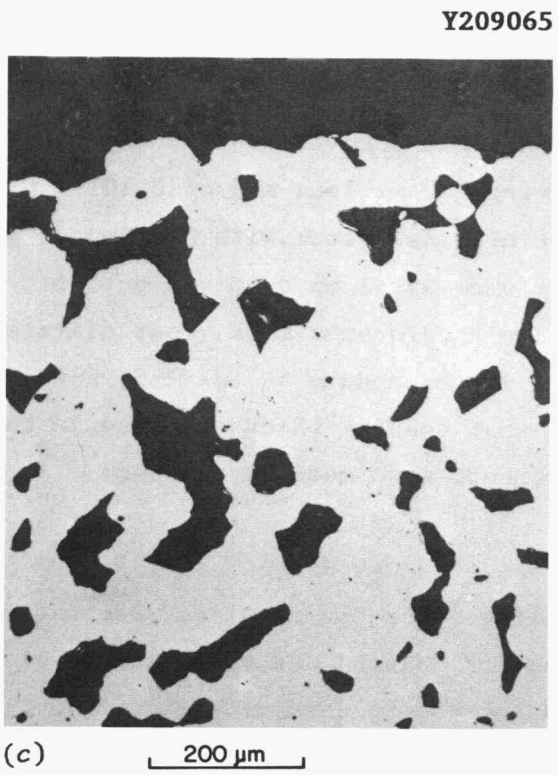

Fig. 1. Polished cross sections of SiC substrate materials.

ORNL-DWG 87M-15977

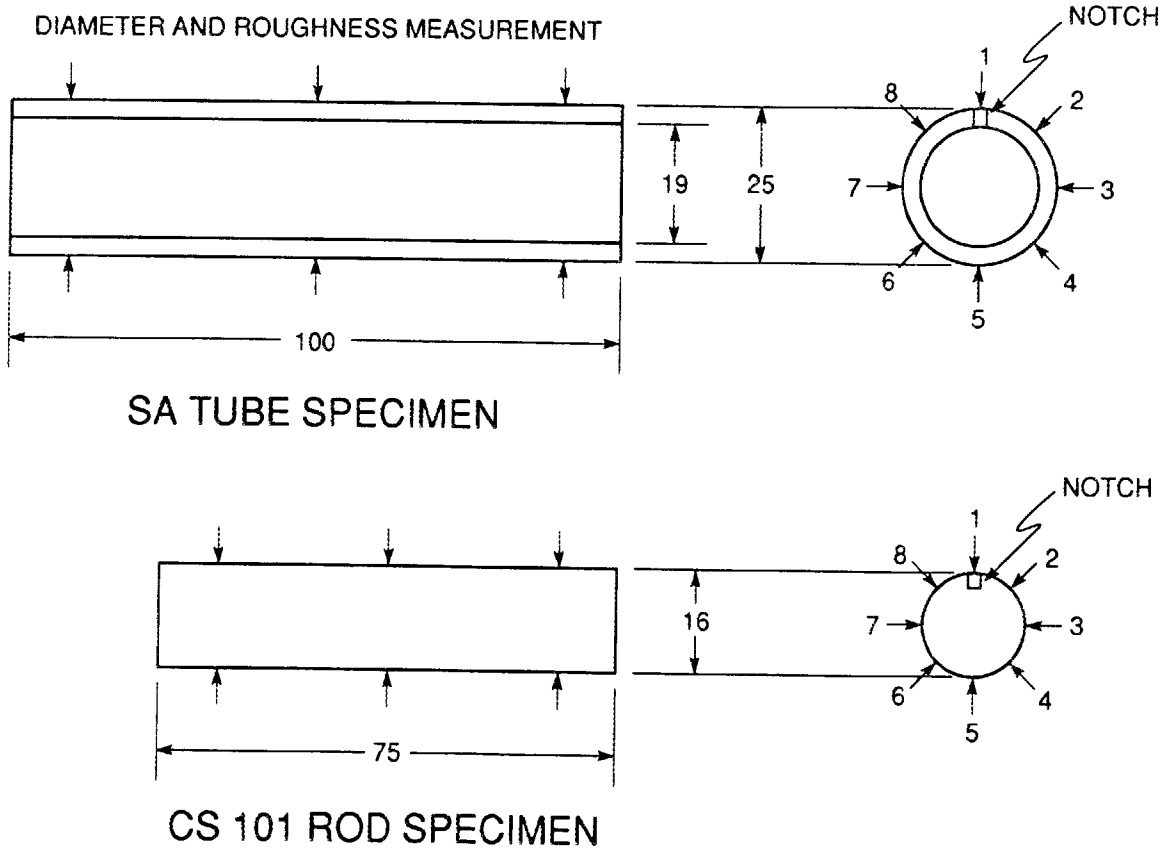

Fig. 2. SA and CS101 specimens showing location of diameter and roughness measurements.

5. APPLICATION OF COATINGS

Several commercial vendors were requested to coat the outer surface of ORNL-provided specimens with selected coatings. Coating materials were also obtained from commercial suppliers for application at ORNL. The coatings were applied by simple dipping, roll dipping (at ORNL), air spraying, and plasma spraying. Brief descriptions of coating methods are presented below.

Dipping. Specimens were submerged in a slurry of the coating material and then removed to allow excess material to drain away. The coating thicknesses and smoothness depended on slurry consistency, drying time, and other factors. After drying in air, the coatings were dried in an oven at ~100°C.

Roll dipping (at ORNL). Each specimen was partially submerged with the long axis horizontal in a slurry and then rotated about the long axis to contact the entire surface with the slurry. The coating thickness and smoothness depended upon slurry consistency, drying time, entrapped air bubbles, mesh size of powder in the slurry, and other factors. Smoother and more uniformly thick coatings were prepared by roll dipping than by simple dipping.

Air spraying. A slurry of coating material was aspirated into the nozzle of an air spray gun and then directed as a fine spray on each specimen rotating about the long axis. The coatings prepared by this method had a surface texture like fine-grit abrasive paper.

Plasma spraying. Conventional plasma spraying was used. Powders of coating materials were fed into the arc discharge of a plasma gun, wherein heating and projection of the powders occurred. The heated powders projected onto each specimen rotating about the long axis. The specimens were heated to ≥1000°C during coating.

6. COATING EVALUATION

The coating evaluation plan is shown in Fig. 3, wherein the principal steps, indicated by numbers, are discussed below.

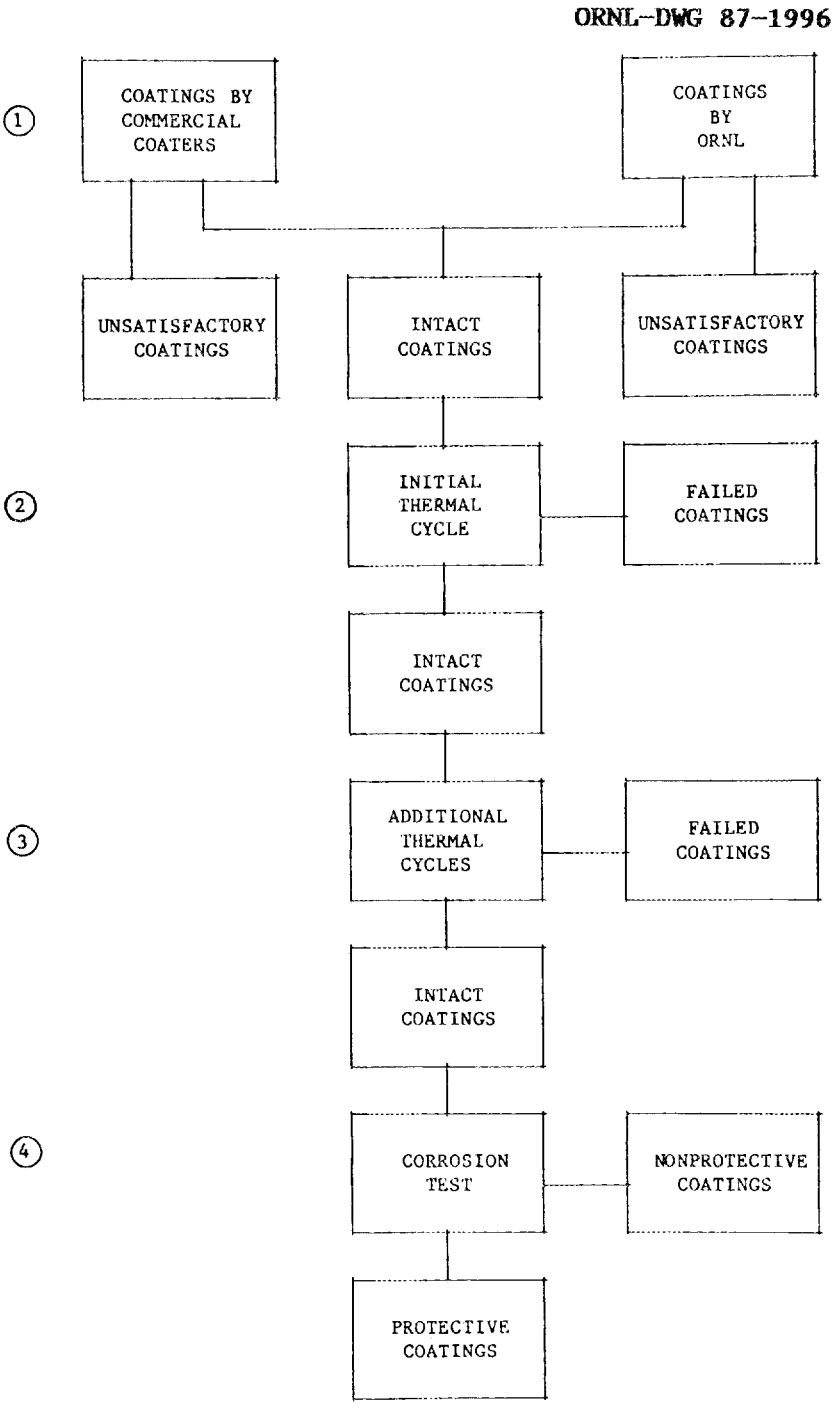

Fig. 3. Coating evaluation plan.

1. The coatings were applied on ORNL-supplied substrate specimens by commercial coaters. Some suppliers of coating materials were unable or unwilling to coat the specimens; therefore, some coatings were prepared at ORNL, using commercially available coating materials. The coatings were visually inspected to determine their suitablity for evaluation. Obviously cracked or spalled coatings were not used.
2. An initial thermal cycle was performed in air as follows:
   25 to 1200°C in 6 h (~200°C/h),
   1200°C for 30 min, and
   1200 to 25°C in 6 h.
   The coatings were again visually inspected to determine their suitability for further evaluation. Most coatings that cracked or spalled were considered to be unsatisfactory for additional thermal-cycle tests.
3. Additional thermal-cycle tests were performed in air at heating and cooling rates of 600°C/h. Afterwards, the coatings were visually inspected to determine their suitability for corrosion testing. Most coatings that cracked or spalled were rejected.
4. Corrosion testing was conducted at 1200°C in an oxidizing atmosphere containing Na_2CO_3. A comparison was made of the corrosion behavior of coated and uncoated specimens.

7. COATING ADHERENCE

The source, coater, designation, and major constituents of the coatings involved in this study are shown in Table 2. Thirty-three coatings based on Al_2O_3, Cr_2O_3, SiO_2, TiO_2, and ZrO_2 were represented, of which 22 were either Al_2O_3- or ZrO_2-based. All thermal expansion coefficients included in Table 2 were greater than those of SiC substrates (5.5×10^{-6}/°C for SA-1 and -2 and 4.8×10^{-6}/°C for CS101). According to the evaluation plan (Fig. 3), the coatings were visually inspected after application to determine their suitability. As will be shown, some coatings cracked and/or detached immediately after application. In fact, some commercial coaters returned uncoated specimens to ORNL because of

Table 2. Coating sources and characteristics

Source	Coated by	Coating	Major constituent(s)	Coefficient of thermal expansion[a] (10^{-6} °C^{-1})	Coating method[b]
Aremco Products, Inc.	Aremco Products, Inc.	Ceramabond 503	Al_2O_3	7.2	D
		Ceramacoat 593	SiO_2	10.8	D
Aremco Products, Inc.	Oak Ridge National Laboratory	Cerama-Dip 538	Al_2O_3	25.2	RD
		Ceramabond 503	Al_2O_3	7.2	RD
		Ceramacoat 593	SiO_2	10.8	RD
		Ultra-Temp 516	ZrO_2	7.4	RD
Ceramic Refractory Corp.	Ceramic Refractory Corp.	C-10A	ZrO_2	(13.5)	AS
		C-90S	ZrO_2	(9.4)	AS
		C-ZS	ZrO_2	(9.4)	AS
Christy Firebrick Co.	Oak Ridge National Laboratory	Alfrax 17A	Al_2O_3	(6.8)	RD
		Morcoset AC	Al_2O_3, Cr_2O_3	(6.8)	RD
Metco, Inc.	Metco, Inc.[c]	Gray alumina 101	Al_2O_3	(6.8)	PS
		White alumina 105	Al_2O_3	(6.8)	PS
		Alumina-titania 130	Al_2O_3	(6.8)	PS
		Alumina-titania 131 VF	Al_2O_3, TiO_2	(7.8)	PS
		Chromium oxide 106	Cr_2O_3	(8.4)	PS
		Chromium oxide-silica 136F	Cr_2O_3	NA	PS
		Chromium oxide-titanium dioxide 111	Cr_2O_3, TiO_2	NA	PS
		Zirconium oxide 201	ZrO_2, CaO	(10.4)	PS
		Zirconium oxide 202 NS	ZrO_2, Y_2O_3	NA	PS
		Magnesium zirconate 210	ZrO_2, MgO	NA	PS
		Calcium zirconate 211	ZrO_2, CaO	NA	PS
RX Chemical Co.	Oak Ridge National Laboratory	RX-14	SiO_2	NA	RD
		RX-21	SiO_2	NA	RD
		RX-36	SiO_2	NA	RD
Sauereisen Cements Co.	Sauereisen Cements Co.	No. 350	SiO_2	NA	D
		No. 360	SiO_2	19.7	D
Sylvester & Co.	Sylvester & Co.[c]	Al_2O_3	Al_2O_3	(6.8)	
		Al_2O_3/TiO_2	Al_2O_3, TiO_2	(6.8)	PS
		Al_2O_3/TiO_2	Al_2O_3, TiO_2	(8.6)	PS
		Spinel	Al_2O_3, MgO	(7.8)	PS
		Cr_2O_3	Cr_2O_3	(8.4)	PS
		Ca stabilized ZrO_2	ZrO_2, CaO	(10.4)	PS
		MgO/ZrO_2	ZrO_2, MgO	NA	PS
		TiO_2	TiO_2	(8.2)	PS
					PS

[a]Values in parentheses are estimated on the basis of major constituent or compound present. NA = not available.

[b]D = dipping, RD = roll dipping, AS = air spraying, PS = plasma spraying.

[c]Specimens were returned uncoated because of nonadherence.

nonadherence of their coatings. Visually satisfactory coatings were subjected to an initial thermal cycle, usually from room temperature to 1200°C, to test for adherence. Subsequently, additional thermal cycles at a faster heating and cooling rate were used as a more severe test of adherence. The two thermal cycles A and B, shown in Fig. 4, had heating and cooling rates of 200 and 600°C/h, respectively. The coatings were visually examined with a binocular microscope at magnifications up to 30x for cracks, detached regions, and other defects before and after thermal cycles. Tables 3–5 show the condition of coatings at various stages. The as-coated condition refers to the dried state in the case of aqueous slurry precursors.

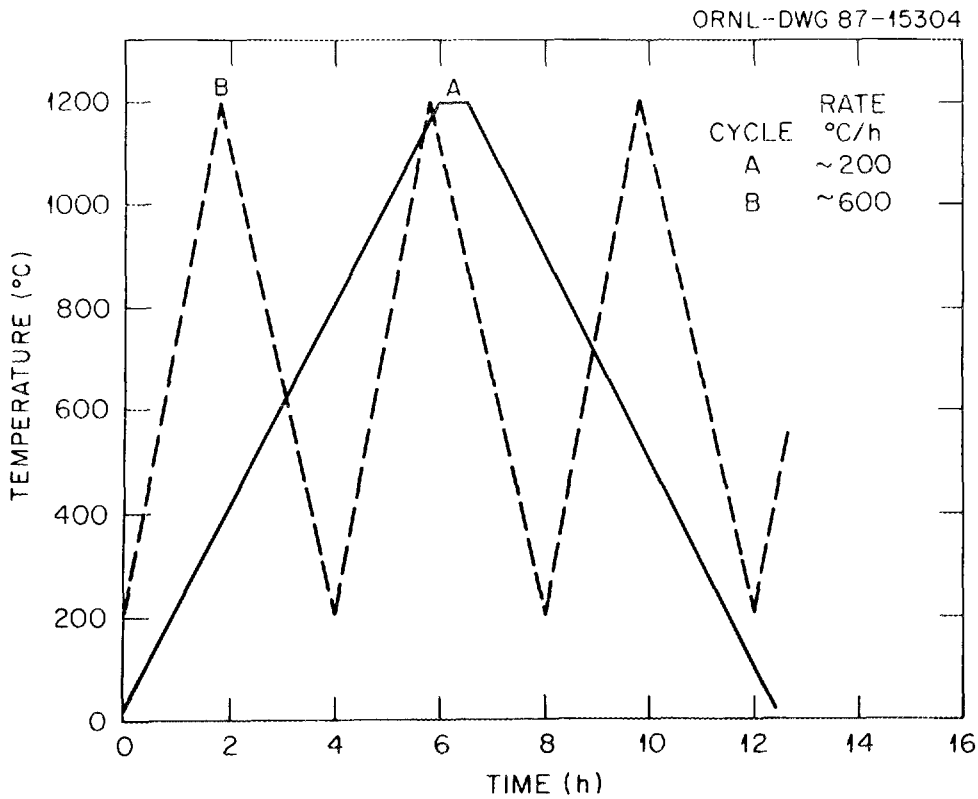

Fig. 4. Thermal cycles used to test coating adherence.

Table 3. Results of adherence tests for Al_2O_3-based coatings

Coating	Substrate	Nominal coating thickness (mm)	Coating condition		
			As-coated[a]	After one A thermal cycle[b]	After indicated number ( ) of B thermal cycles[b]
Cerama-Dip 538	SA		Cracked, partially spalled	Completely spalled	
Cerama-Dip 538	CS101		Satisfactory	Circumferencial and longitudinal cracks, shrank exposing substrate	(55) Cracked, shrank, partially spalled
Ceramabond 503	SA		Cracked	Cracked, partially spalled	
Alfrax 17A	SA	0.3	Satisfactory	Numerous small cracks	(59) Numerous small cracks, particles missing
Alfrax 17A	CS101	0.2	Satisfactory	Numerous small cracks	(55) Numerous small cracks, particles missing
Morcoset AC	SA	0.3	Satisfactory	Several small cracks at ends	(59) Cracked, partially detached
Morcoset AC	CS101	0.2	Satisfactory	Several cracks	(55) Several cracks, not changed from first cycle

[a]After drying in air at room temperature or at 110°C in the case of aqueous slurry precursors.

[b]See Fig. 4.

Table 4. Results of adherence tests for SiO_2-based coatings

Coating	Substrate	Nominal coating thickness (mm)	Coating condition		
			As-coated[a]	After one A thermal cycle[b]	After indicated number ( ) of B thermal cycles[b]
Ceramacoat 593	SA		Cracked, partially spalled	Completely spalled	
Ceramacoat 593	CS101		Satisfactory	Cracked, blistered	(55) Cracked, blistered, shrank, partially spalled
RX-14	SA	0.2	Satisfactory	Partially spalled, glassy with bubbles	
RX-21	SA	0.3	Satisfactory	Glassy, incomplete wetting, partially spalled	
RX-36	SA	0.6	Satisfactory	Glassy, separated into thick and thin regions	
No. 350	SA	2–3	Satisfactory except nonuniform thickness	Longitudinal crack entire length, partially spalled	
No. 360	SA	2	Satisfactory except nonuniform thickness	Longitudinal crack at one end	(53) Shrank, longitudinal crack entire length, debonded, numerous small holes extending to substrate

[a]After drying in air at room temperature or at 110°C in the case of aqueous slurry precursors.

[b]See Fig. 4.

Table 5. Results of adherence tests for ZrO_2-based coatings

Coating	Substrate	Nominal coating thickness (mm)	Coating condition		
			As-coated[a]	After one A thermal cycle[b]	After indicated number ( ) of B thermal cycles[b]
Ultra-Temp 516	SA		Satisfactory	Completely spalled	
Ultra-Temp 516	CS101		Satisfactory	Circumferential and longitudinal cracks	(55) Completely spalled
C-10A	SA	<0.1	Satisfactory	Satisfactory	(50) Detached on one end
C-90S	SA	0.1	Satisfactory	Satisfactory	(50) Satisfactory except a 5-mm-diam area of small cracks
C-ZS	SA	0.1	Satisfactory	Satisfactory	Satisfactory

[a]After drying in air at room temperature or at 110°C in the case of aqueous slurry precursors.

[b]See Fig. 4.

7.1 Al_2O_3-BASED COATINGS

The results for Al_2O_3-based coatings are shown in Table 3. Cerama-Dip 538/SA (RD) and Ceramabond 503/SA (RD)* spalled extensively during one A thermal cycle. Cerama-Dip 538/CS101 (RD) had circumferential and longitudinal cracks and exhibited shrinkage after one A thermal cycle (Fig. 5). Alfrax 17A/SA (RD) had numerous small cracks after one A thermal cycle. After 59 B thermal cycles, the coating was still intact (Fig. 6); however, some coarse particles had detached, leaving pits. Substantially the same results were obtained when Alfrax 17A was coated on CS101 substrates. Morcoset AC/SA (RD) had several small cracks after one A thermal cycle, but it partially detached during 59 B thermal cycles (Fig. 6). Morcoset AC/CS101 (RD) developed several cracks during one A thermal cycle, but it did not degrade further during 55 B thermal cycles. As shown in Table 3, Alfrax 17A and Morcoset C had nominal coating thicknesses of 0.3 and 0.2 mm (0.012 and 0.008 in.), respectively. The effect of coating thickness on adherence has not been determined.

Thus, two Al_2O_3-based coatings, Morcoset AC and Alfrax 17A, remained intact, although cracked, after thermal-cycle tests for adherence. Cracks might not be critical to coating performance if the Al_2O_3 sufficiently increases the refractoriness of the silicate reaction product. Under this proposition, the corrosive atmosphere might gain access to the SiC (SiO_2 film) through cracks in the coating, but the resulting reaction product involving Al_2O_3 would inhibit further reaction. Morcoset AC and Alfrax 17A, therefore, were subjected to corrosion testing.

7.2 SiO_2-BASED COATINGS

The results of adherence tests for SiO_2-based coatings are shown in Table 4. These coatings would be beneficial during corrosion only if the content of compounds such as Al_2O_3, Cr_2O_3, TiO_2, and ZrO_2 were sufficiently high to increase the refractoriness of the reaction product. Ceramacoat 593/SA (RD) cracked and partially spalled during drying immediately after coating. Ceramacoat 593/CS101 (RD) cracked and blistered after one A thermal cycle, and partially spalled after 55 B thermal cycles. Coatings RX-14, RX-21, and RX-36 have specific glazing

---

*/SA or /CS101 refers to the substrate material. The designation in parentheses refers to the coating method (e.g., RD means roll dipping).

ORNL-PHOTO 6262-87

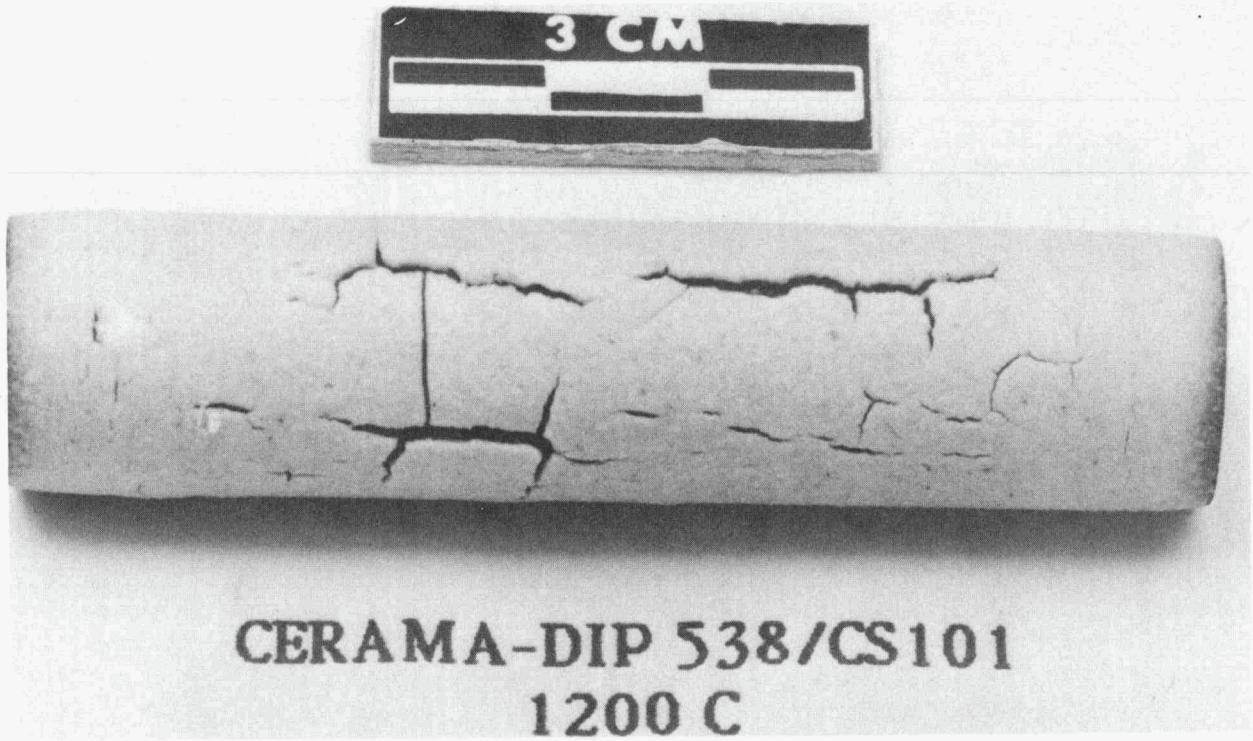

Fig. 5. Cerama-Dip 538/CS101 after one A thermal cycle.

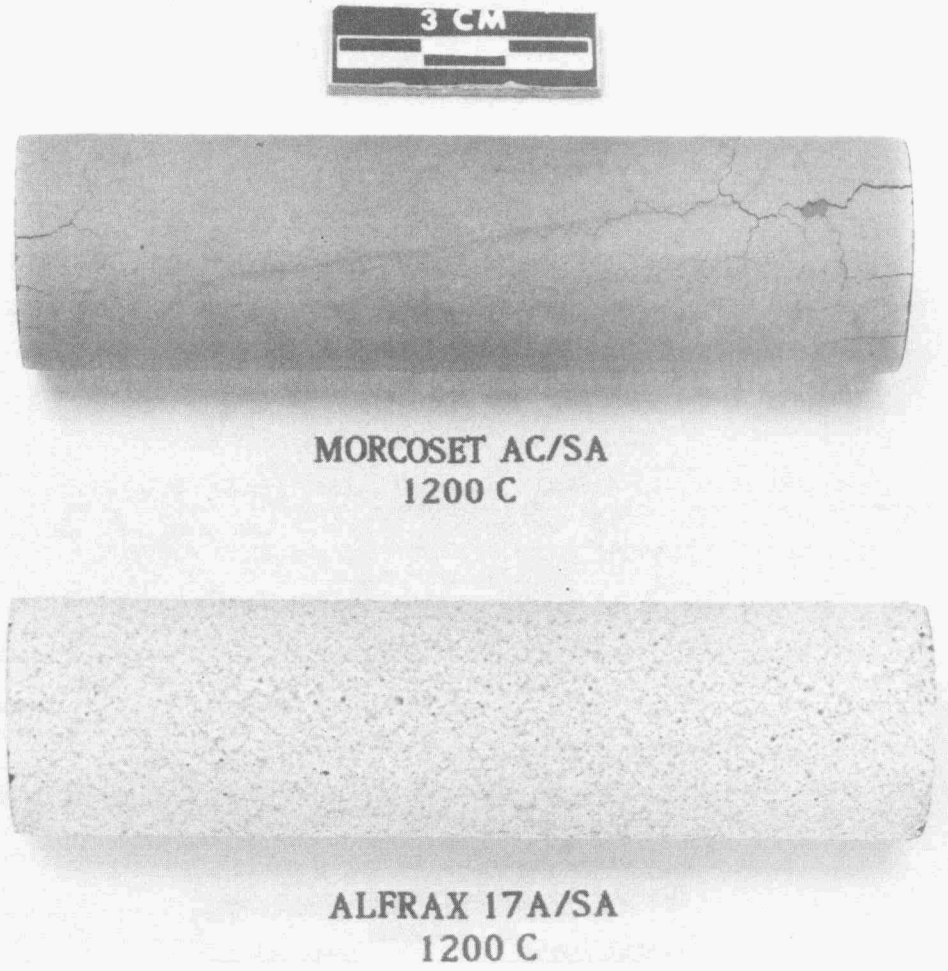

Fig. 6. Morcoset AC/SA and Alfrax 17A/SA after 59 B thermal cycles.

temperatures. When coating RX-14/SA (RD) was heated to the glazing temperature of 760°C, partial spalling occurred. Subsequent heating to 1150°C caused formation of a cracked, glassy coating containing gas bubbles (Fig. 7). Coating RX-21/SA (RD) did not wet the substrate when heated to the glazing temperature of 1150°C. Subsequent heating to 1480°C caused part of the coating to flow off of the specimen (Fig. 8). Coating RX-36/SA (RD) formed a nonuniformly thick glassy coating when heated to the glazing temperature of 1480°C (Fig. 9). Silicate glass coatings, as discussed in Sect. 2, do not protect SiC from oxidation at high temperatures. Consequently, these coatings are not candidates for corrosion protection, even though they are somewhat adherent.

Coatings 350/SA (D) and 360/SA (D) exhibited cracking and spalling, as shown in Fig. 10. As a result of these adherence tests, none of the SiO_2-based coatings appear to be suitable for coating SiC.

7.3 ZrO_2-BASED COATINGS

The results of adherence tests for ZrO_2-based coatings are shown in Table 5. Ultra-Temp 516/SA (RD) spalled completely after one A thermal cycle, while Ultra-Temp 516/CS101 (RD) spalled completely during 55 B thermal cycles. Coating C-10A/SA (AS) partially detached during 50 B thermal cycles (Fig. 11); however, C-90S/SA (AS) and C-ZS/SA (AS) survived with little or no visual degradation (Figs. 12 and 13). The C-10A, C-90S, and C-ZS coatings appeared to be uniformly thick (~0.1 mm), with a texture similar to 600-grit emery paper. Coatings C-90S and C-ZS, therefore, were subjected to corrosion testing. None of the other ZrO_2-based coatings had satisfactory adherence.

8. CORROSION TESTING

Several coatings that survived 50 or more B thermal cycles were subjected to corrosion testing in an oxidizing atmosphere containing Na_2CO_3. Two Al_2O_3-based coatings, Morcoset AC and Alfrax 17A, remained intact, although they cracked during the thermal-cycle tests. Two

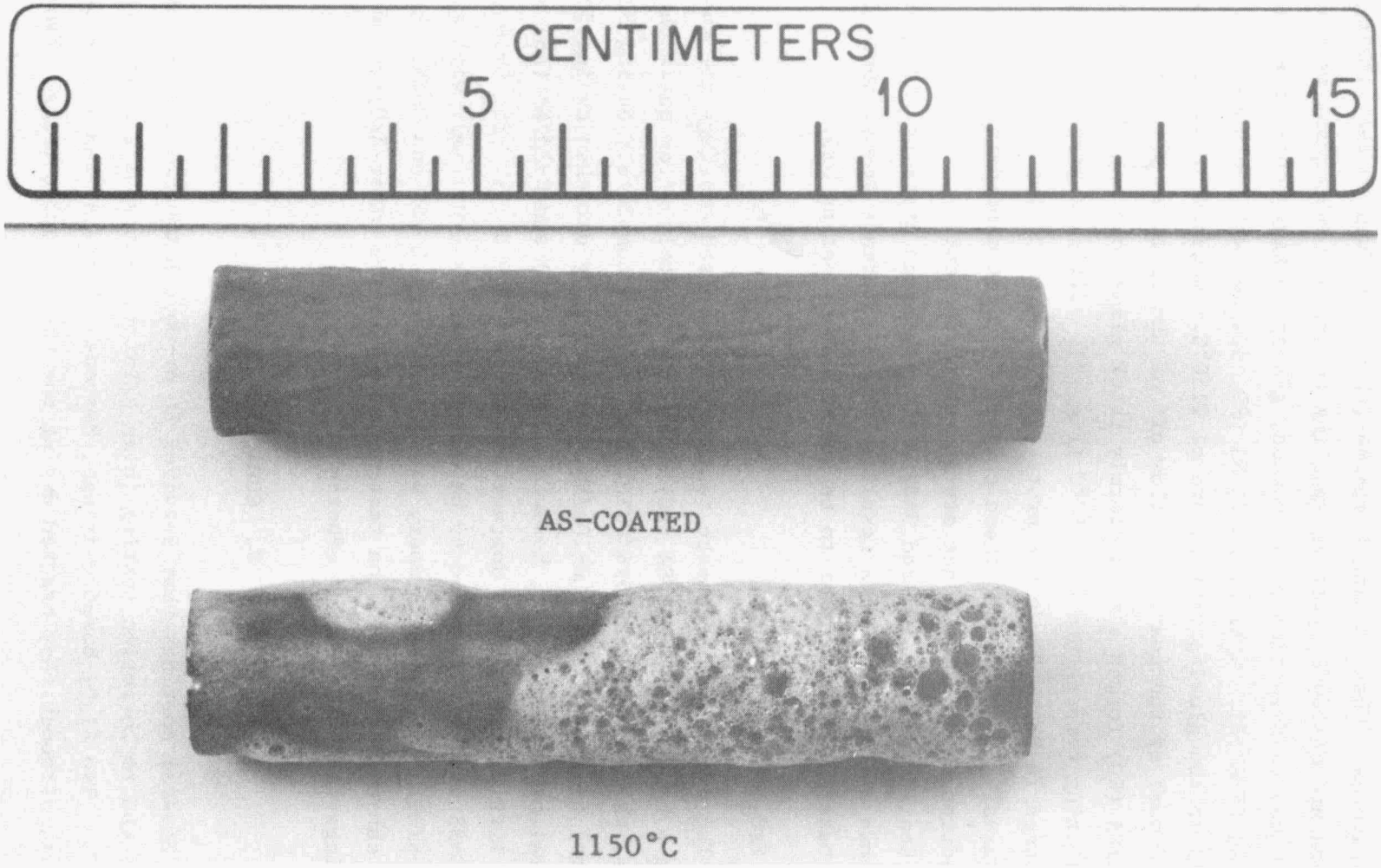

Fig. 7. RX-14/SA after one thermal cycle to 1150°C.

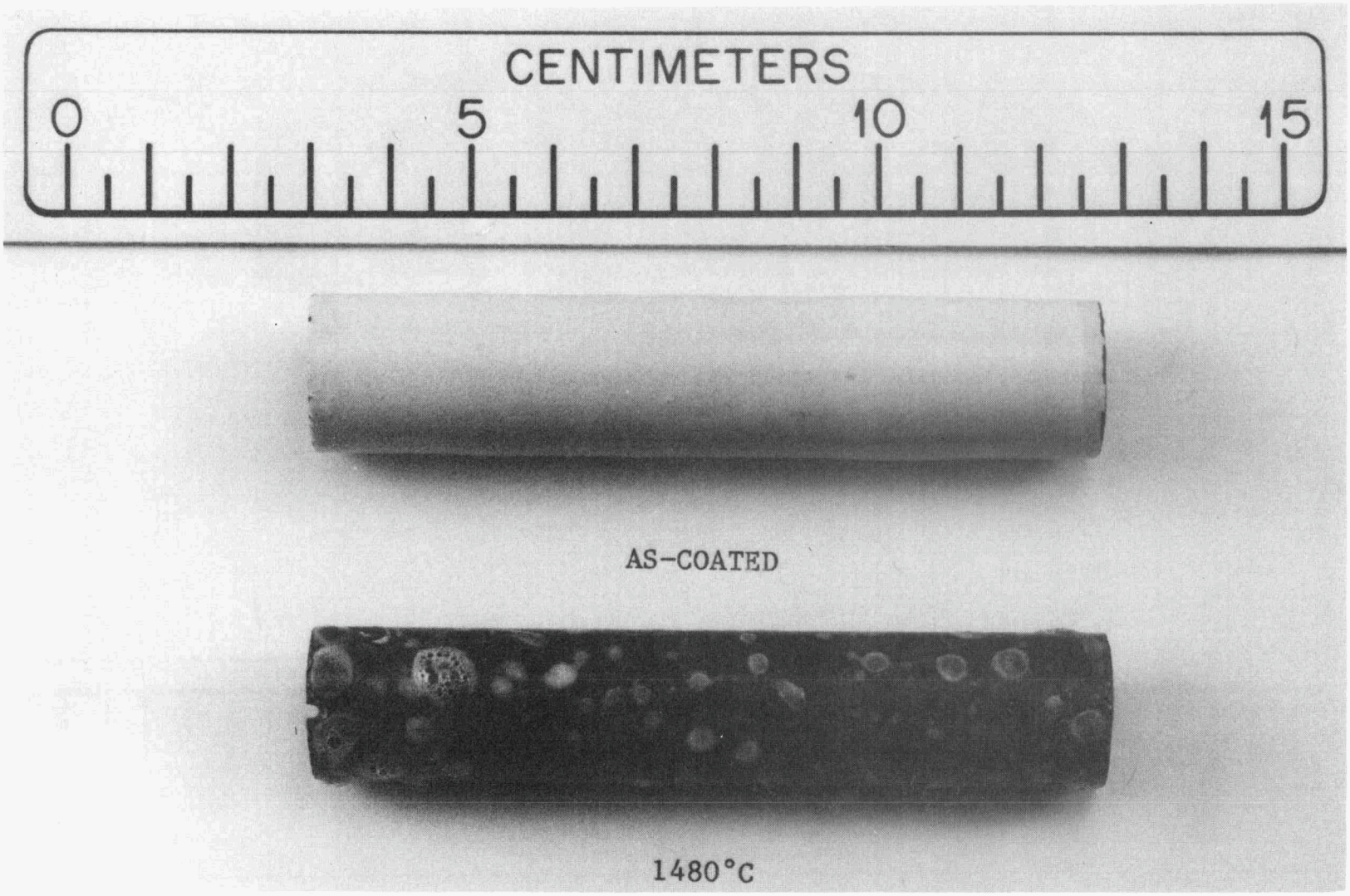

Fig. 8. RX-21/SA after one thermal cycle to 1480°C.

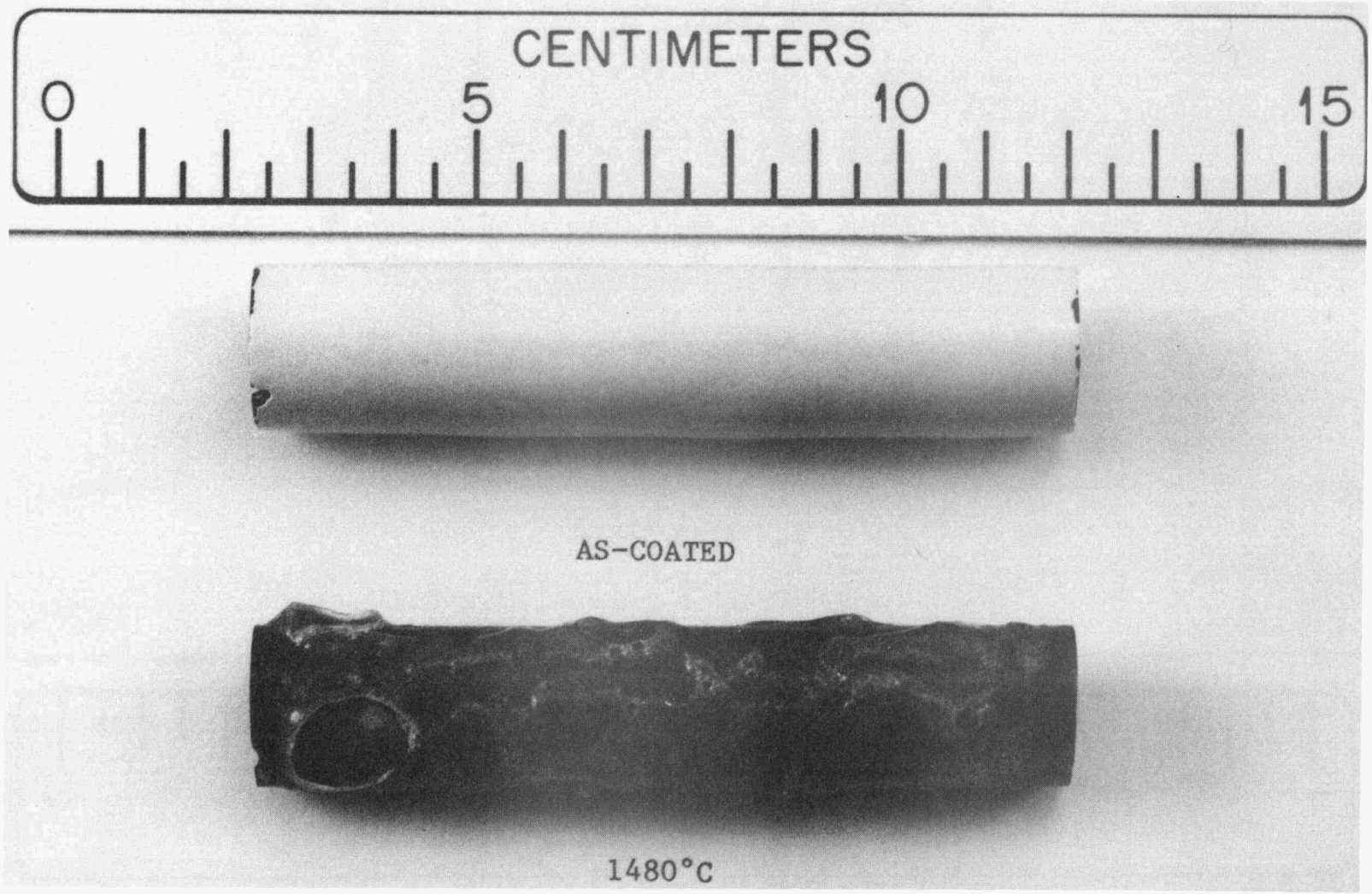

Fig. 9. RX-36/SA after one thermal cycle to 1480°C.

ORNL-PHOTO 6260-87

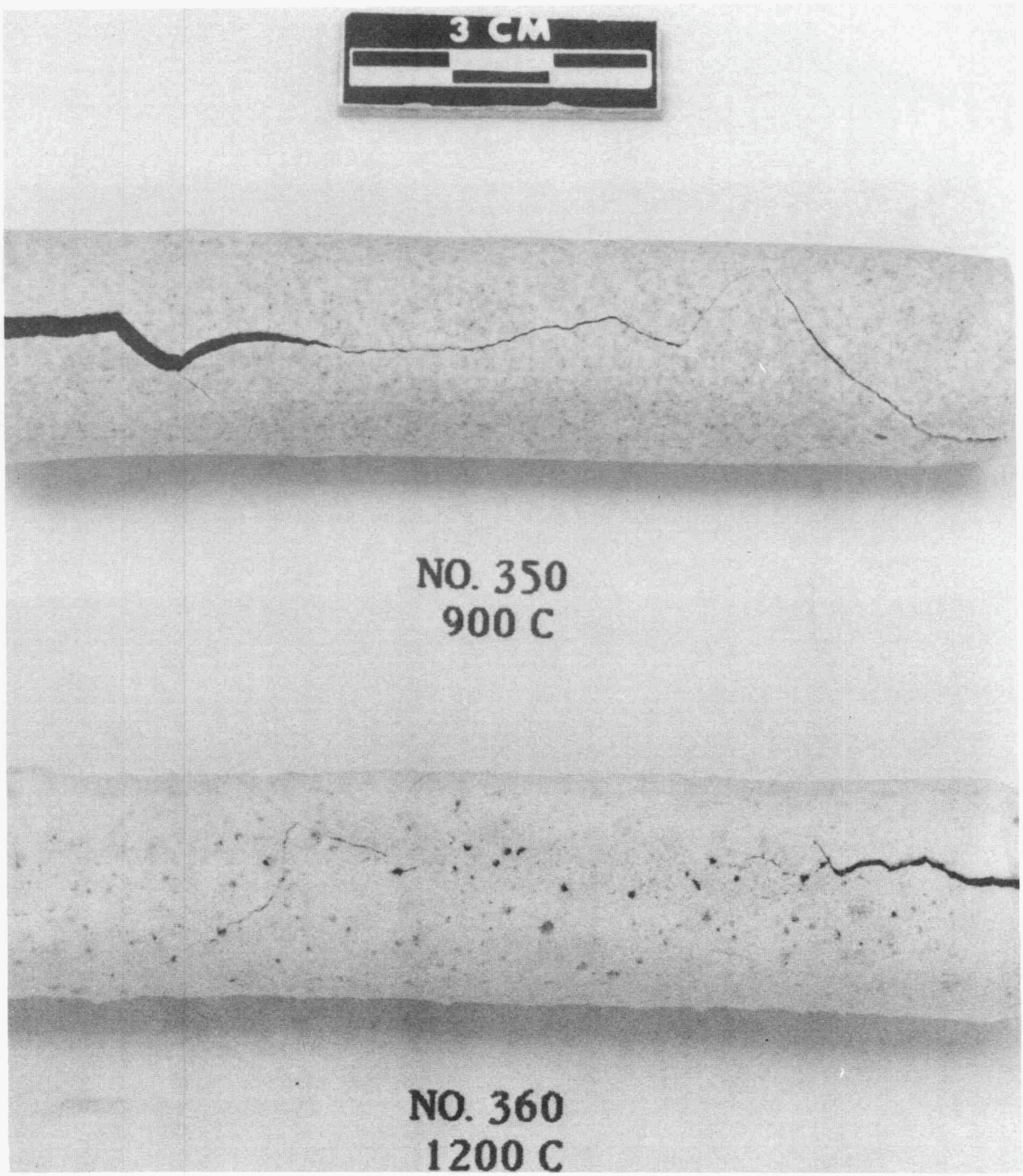

Fig. 10. 350/SA after one thermal cycle to 900°C and 360/SA after 53 B thermal cycles.

ORNL-PHOTO 5857-87

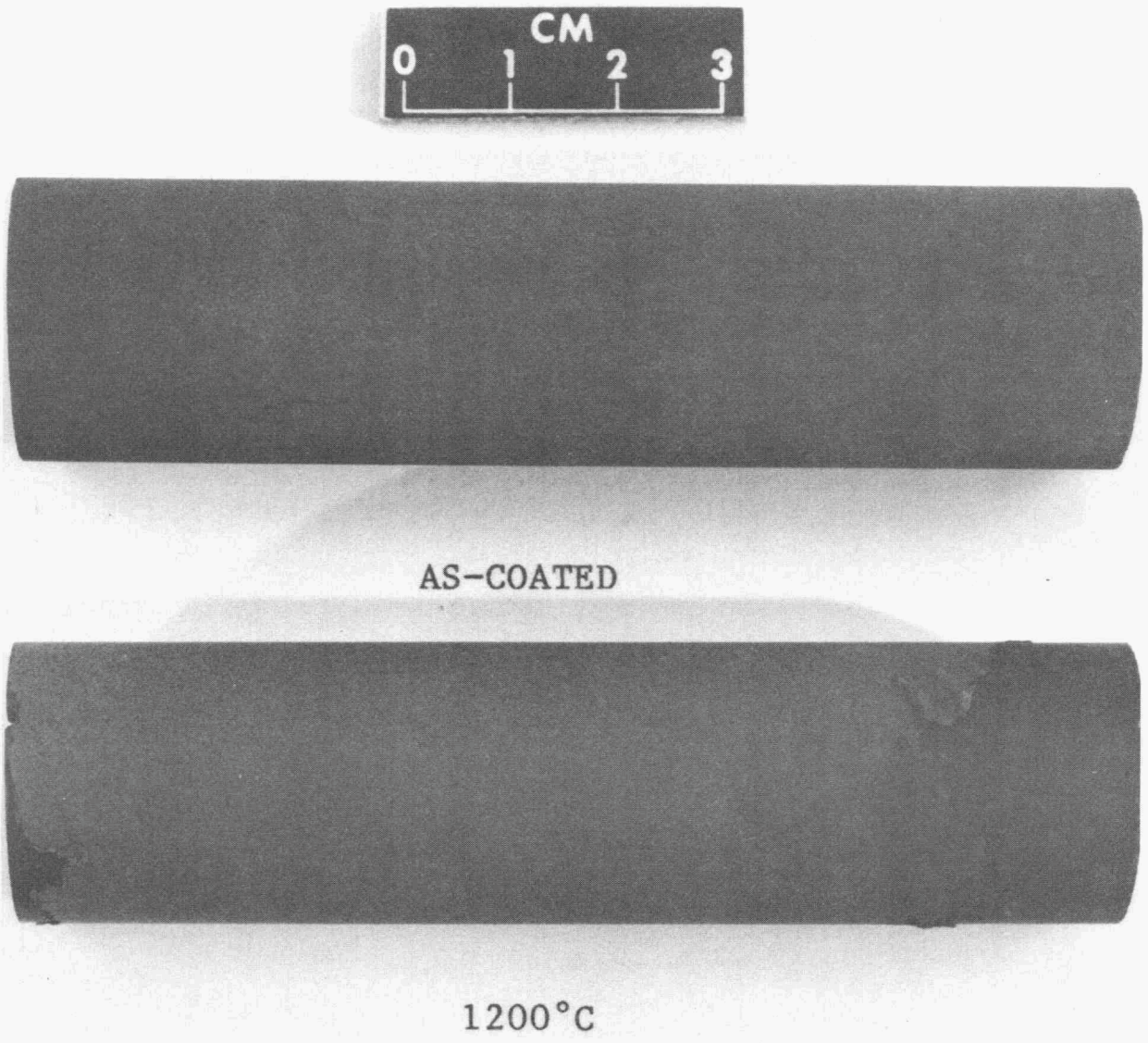

Fig. 11. C-10A/SA after 50 B thermal cycles.

ORNL-PHOTO 2326-87

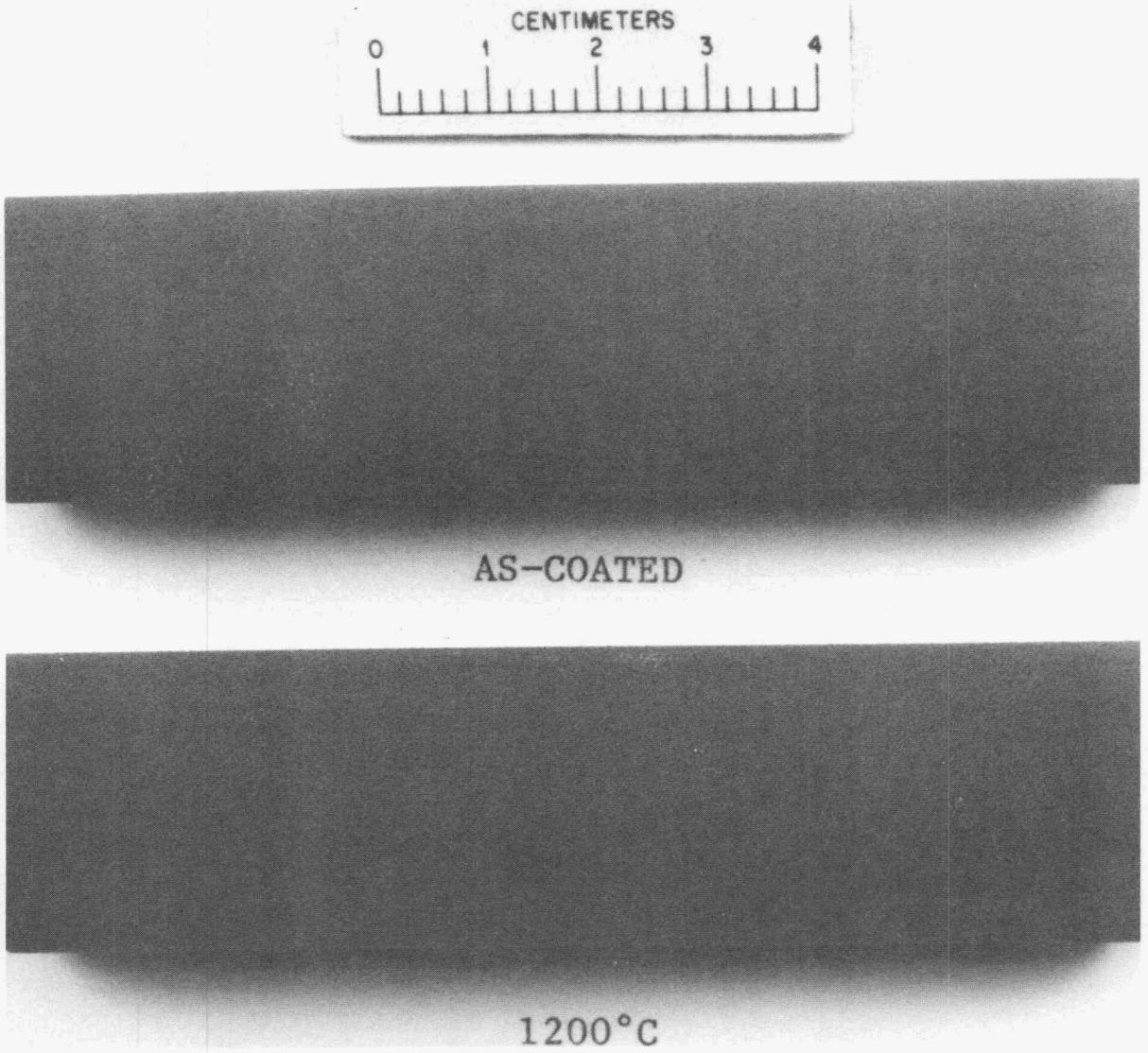

Fig. 12. C-90S/SA after 50 B thermal cycles.

ORNL-PHOTO 2325-87

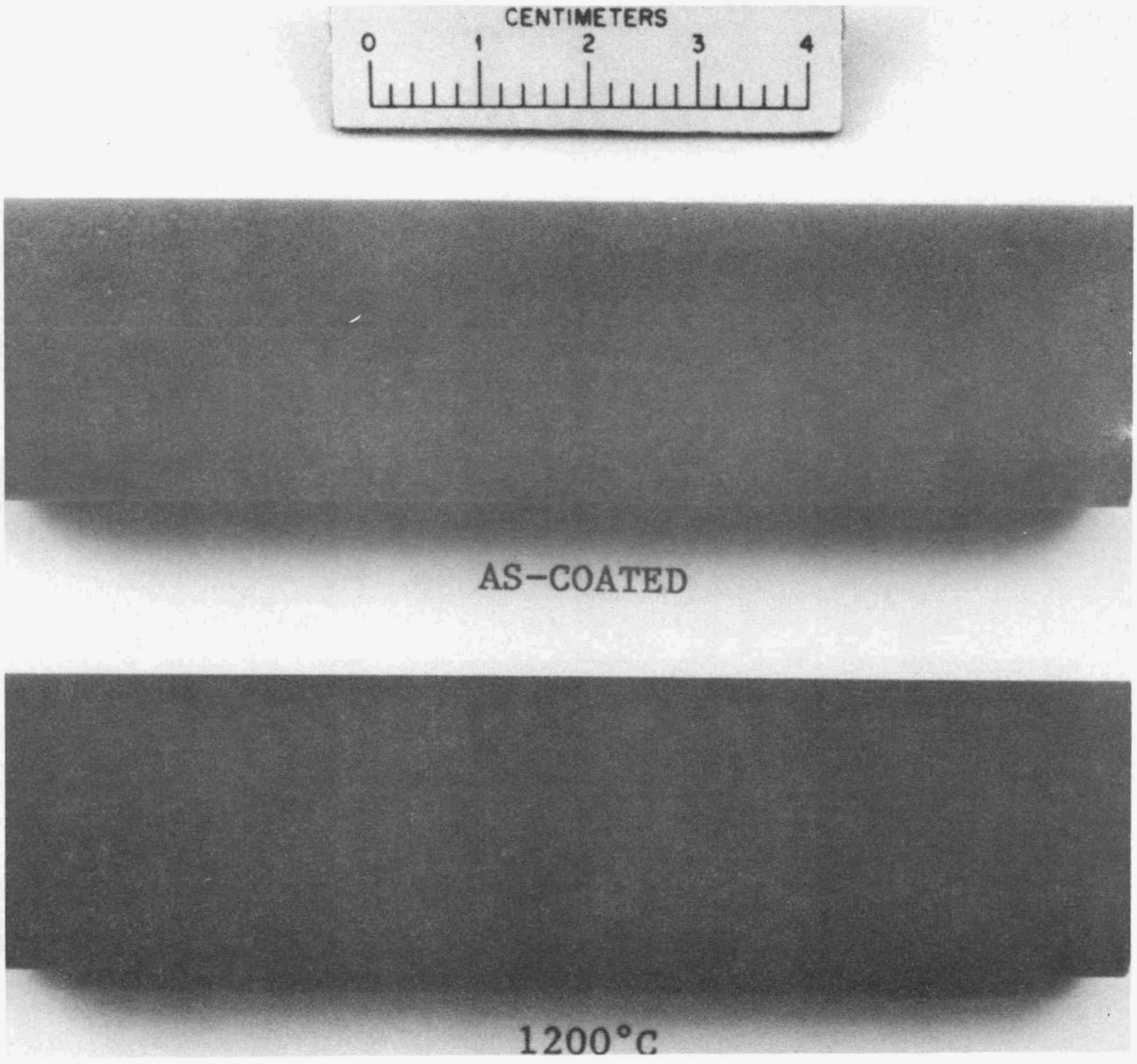

Fig. 13. C-ZS/SA after 50 B thermal cycles.

ZrO_2-based coatings, C-90S and C-ZS, remained intact without cracks. The purpose of the corrosion test was to show that the coatings could protect SiC under conditions known to be corrosive to uncoated SiC.

The test apparatus (Fig. 14) consisted mainly of an alumina tube heated by a furnace, a specimen holder, and a platinum evaporator cup. Air and a solution of H_2O-1 wt % Na_2CO_3 were metered into the top of the alumina tube. Drops of the solution fell into the platinum cup, where evaporation occurred. Vapors of H_2O and Na_2CO_3 (or their reaction products) passed through small holes in the wall of the cup and mixed with air. The gas mixture contacted the specimen enroute to the exit at the bottom of the tube. The specimen was located about 25 mm below the cup. Although the control thermocouple was located on the outer wall of the furnace tube, another thermocouple temporarily located inside the tube showed that the temperature was 1200 ± 10°C over a 13-cm length that included the specimen and cup.

Corrosion testing was conducted at 1200°C and 0.1 MPa (1 atm). Table 6 shows that the gas mixture contained only 0.05 wt % Na_2CO_3 along with the other main constituents. Specimens were heated to 1200°C in ~6 h with air flowing. At ~500°C, pure H_2O was metered into the evaporator cup. Upon reaching 1200°C, the H_2O-1 wt % Na_2CO_3 solution replaced pure H_2O. After a test duration of 48 h, the solution was replaced by pure H_2O and the furnace was cooled to room temperature in about 8 h.

The appearance of uncoated SA-1 specimens (sections of SA-1 tube) before and after the corrosion test are shown in Fig. 15. The test caused a decrease in thickness of 0.9 mm and unmeasured, though noticeable, decreases in length and width also. The test conditions were quite corrosive to uncoated SiC. Figures 16 and 17 show coated specimens before and after testing. The coatings obviously did not protect the SiC substrates. The Alfrax 17A coating was completely consumed by reaction, and only part of the Morcoset AC coating remained (Fig. 16). Both specimens had a glassy deposit (reaction product) that appeared to have been molten at the test temperature and partially wet the surface. Specimens coated with the two ZrO_2-based materials were also covered with

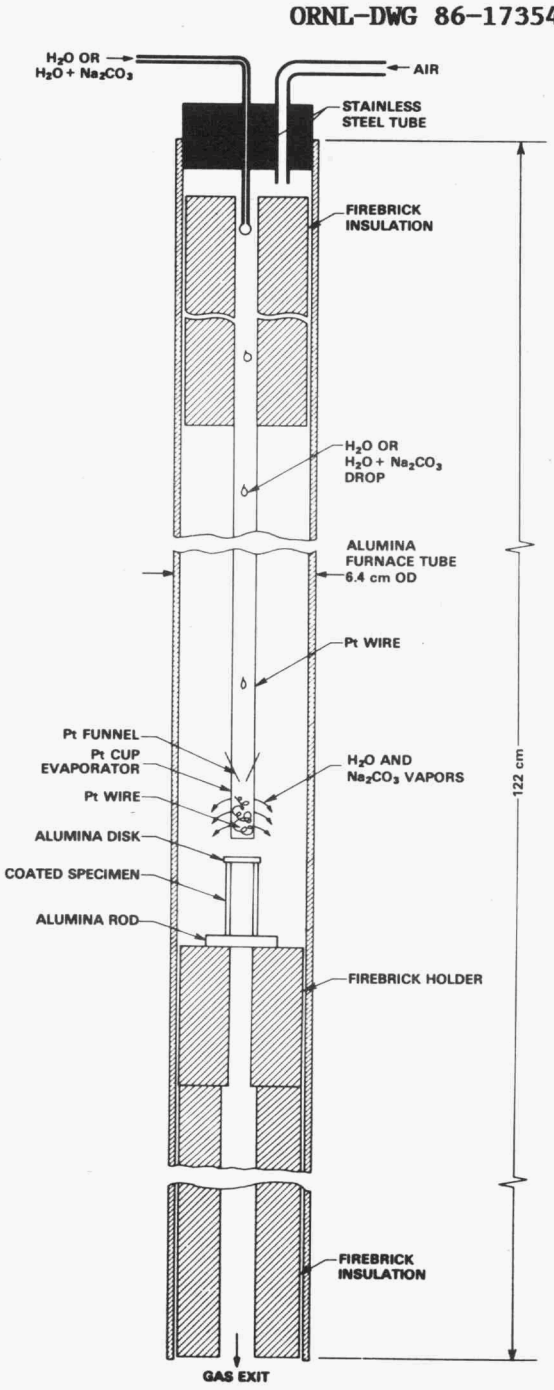

Fig. 14. Schematic of apparatus for corrosion testing coated specimens.

Table 6. Composition of gas used for corrosion tests

	Flow rate			Composition (wt %)
	cm^3/min at 20°C	cm^3/min at 1200°C	g/min	
N_2	4,930	24,370	5.64	73
O_2	1,310	6,475	1.71	22
H_2O	*a*	2,420	0.36	5
Na_2CO_3	*a*	5	0.004	0.05

[a]Metered as H_2O–1 wt % Na_2CO_3 solution into an evaporator cup at 1200°C.

ORNL-PHOTO 6371-87

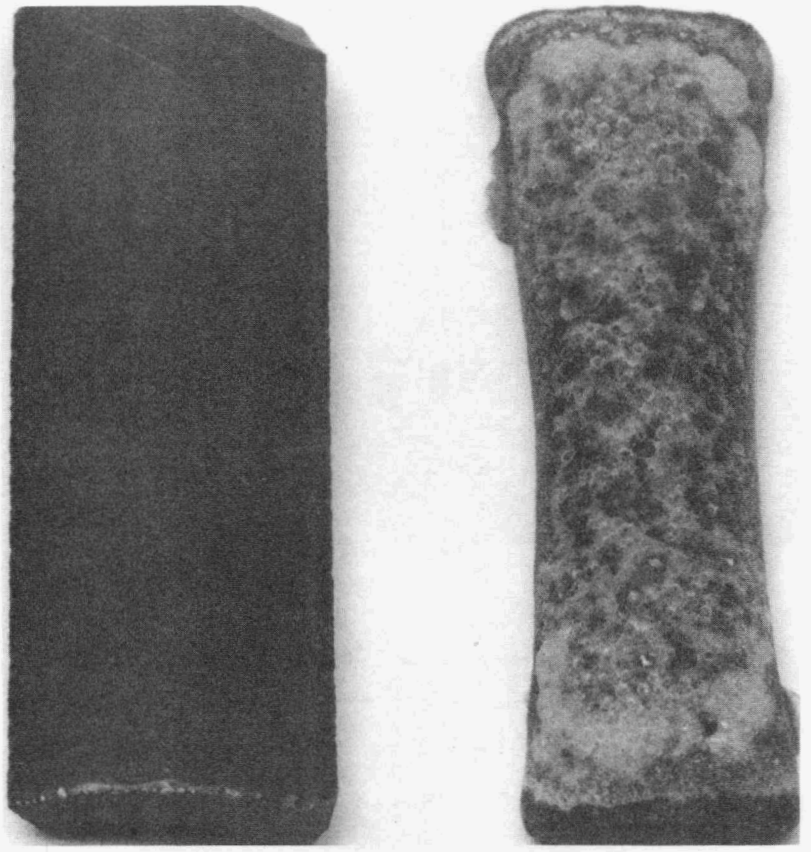

Fig. 15. SA-1 substrate specimen before and after corrosion test.

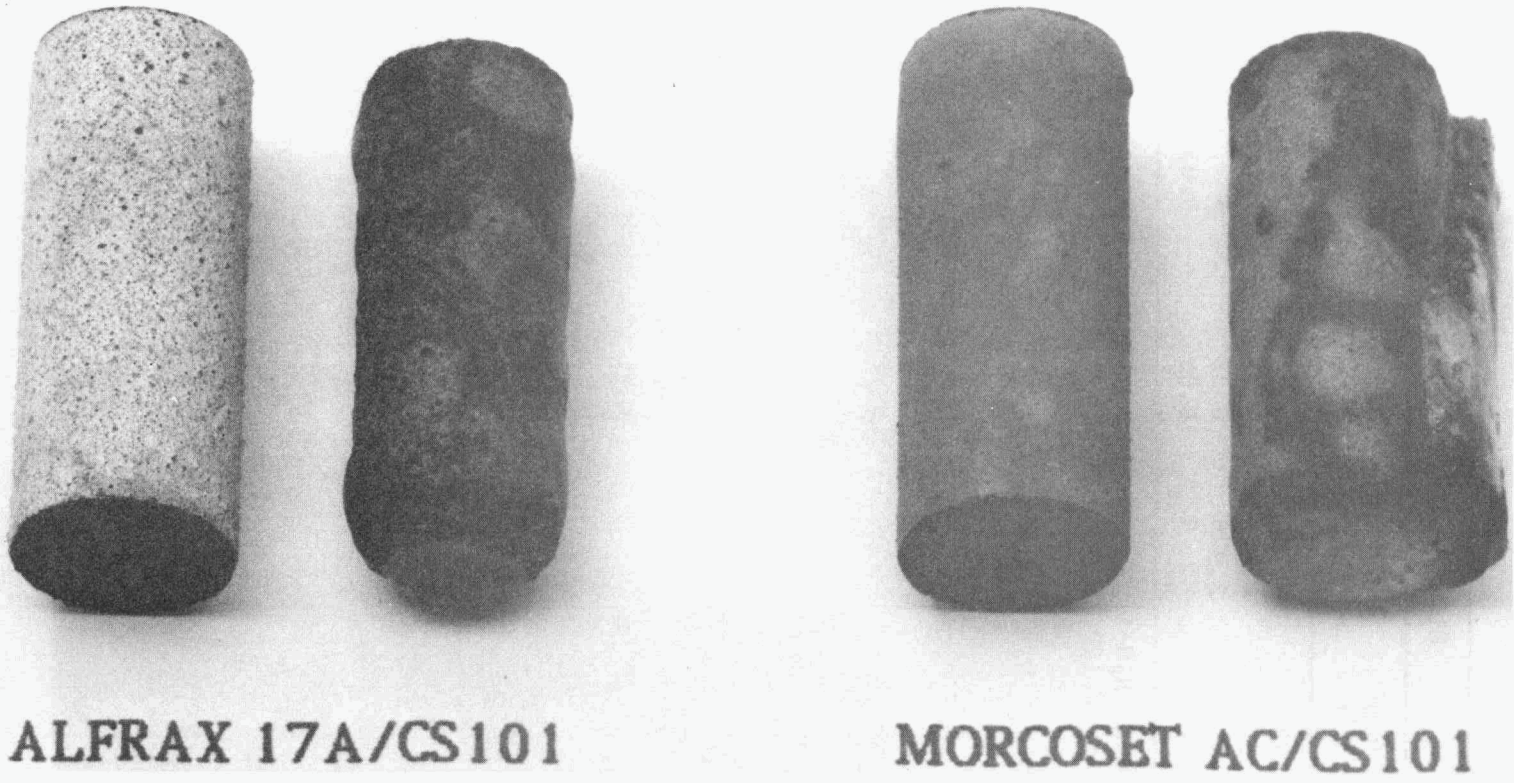

Fig. 16. Alfrax 17A and Morcoset AC coatings before and after corrosion test.

a glassy reaction product. During the test, the C-90S/SA specimen sat in an Al_2O_3 dish. After the test, the dish contained a considerable quantity of glass, which is visible in Fig. 17. The C-ZS/SA specimen sat on Al_2O_3 rods, which allowed the glass to drain.

The glass was dissolved from a portion of the specimens with hydrofluoric acid to permit diameter measurements. Control samples showed that the acid treatment did not significantly affect the SiC substrates. Corrosion caused the surface recessions shown in Table 7. Although the coatings did not provide the desired protection, the coated specimens corroded less than uncoated SA-1. The results indicate that the presence of Al_2O_3 or ZrO_2 in the corrosion product decreased the corrosion rate and that better coatings would significantly improve the corrosion resistance.

The microstructures of the coatings suggest reasons for the poor corrosion resistance. The microstructures of Morcoset AC and Alfrax 17A are shown in Figs. 18(*a*) and 18(*c*), respectively. The coatings were about 0.2 mm (0.008 in.) thick and were quite porous. Both coatings penetrated some of the pores at the surface of the CS101 substrates, which probably improved their adherence during thermal cycling (compared with SA-1 substrates), as indicated in Table 3. The coatings, especially Alfrax 17A, were also cracked, as previously mentioned. The corrosion atmosphere readily penetrated the coatings and reacted with the substrates to form glassy, low-melting reaction products. The reaction product tended to fill pores near the surface, as shown in Figs. 18(*b*) and 18(*d*). Much of the reaction product drained from the specimens during the test.

The microstructures of coatings C-90S and C-ZS are shown in Figs. 19(*a*) and 19(*c*), respectively. These coatings were only ~0.1 (0.004 in.) thick and quite porous. Neither provided the desired protection during the corrosion test. As a result, the SA-1 substrates corroded to form the glassy reaction products in Figs. 19(*b*) and 19(*d*).

9. DISCUSSION AND SUMMARY

The ceramic coatings in this study exhibited mostly poor adherence to SiC substrates. Coatings adhere because of mechanical or chemical

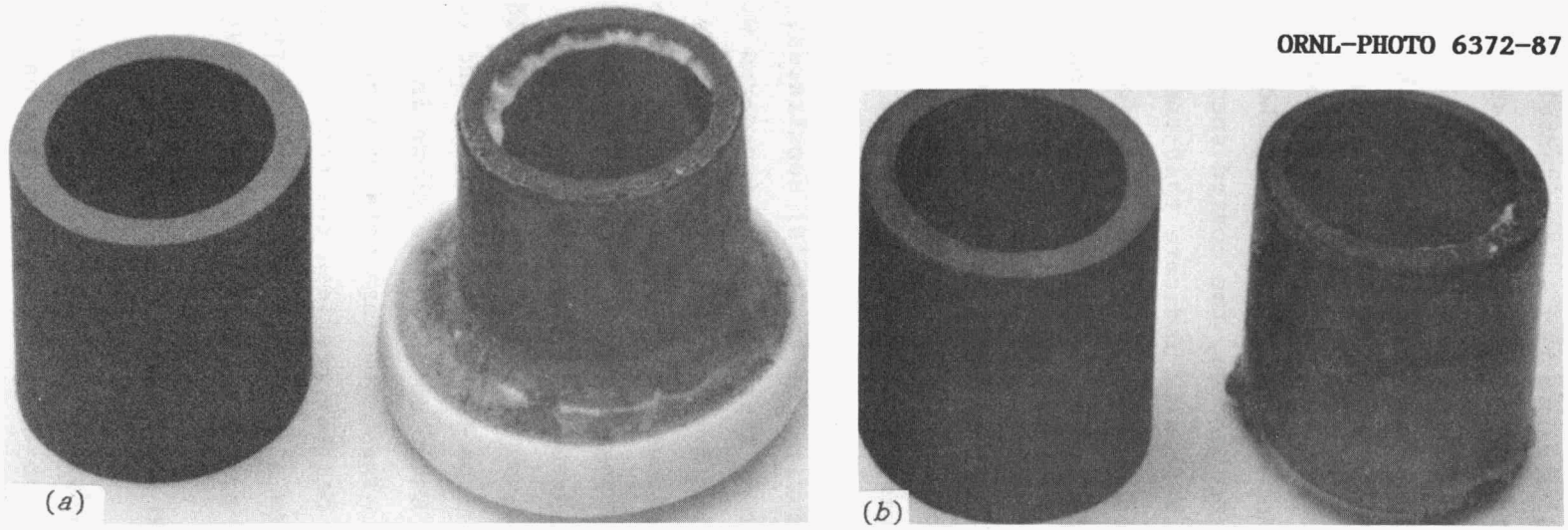

Fig. 17. (*a*) C-90S and (*b*) C-ZS coatings before and after corrosion test.

Table 7. Results of corrosion tests

	Diameter or thickness		Surface recession (mm)
	Before (mm)	After (mm)	
SA-1 (uncoated)	3.92	2.08	0.9
Alfrax 17A/CS101	16.5	15.4	0.6
Morcoset AC/CS101	16.4	15.7	0.4
C-90S/SA	25.4	24.8	0.3
C-ZS/SA	25.3	24.4	0.5

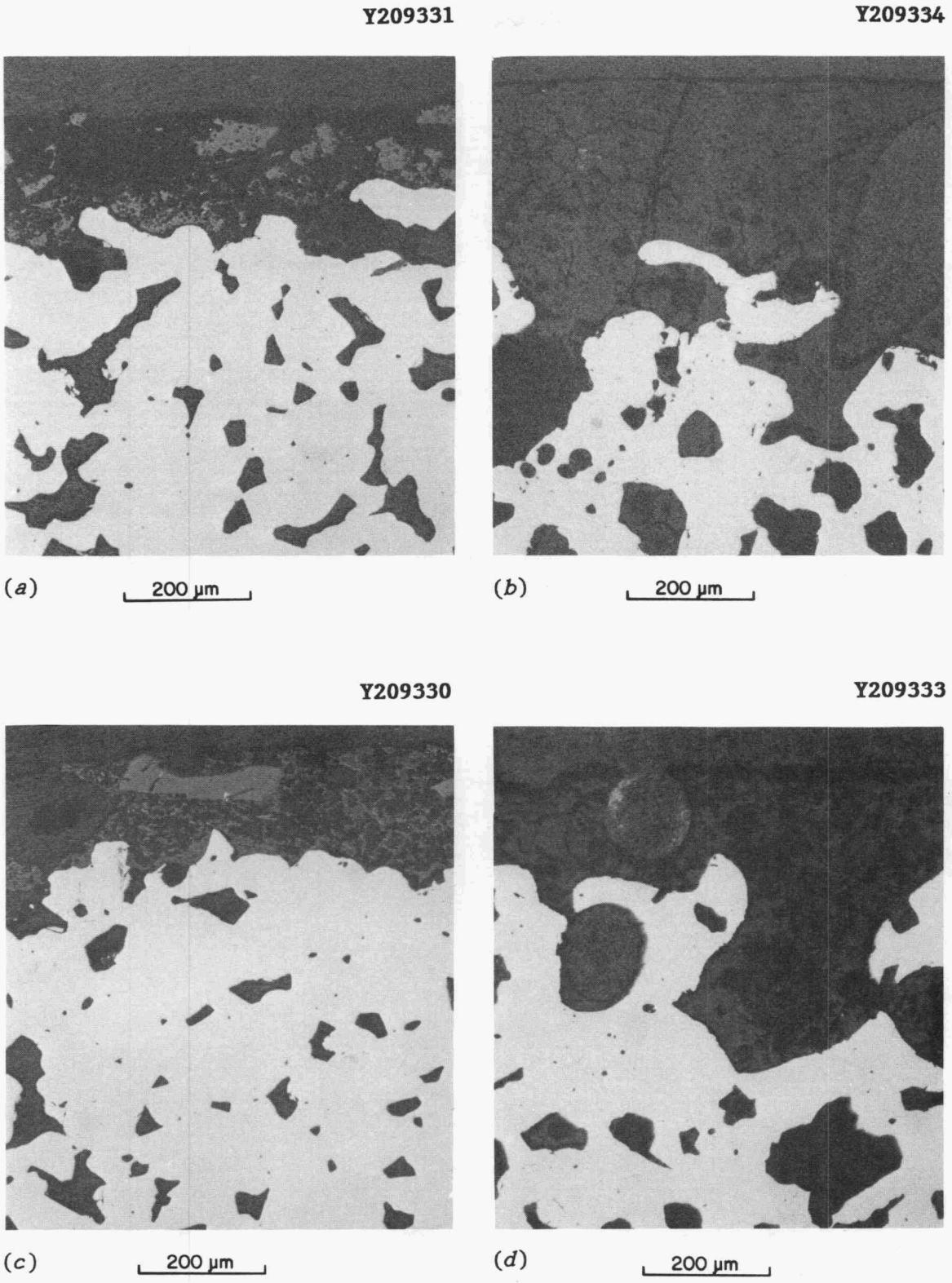

Fig. 18. Microstructures of Morcoset AC/CS101 and Alfrax 17A/CS101 before and after corrosion test. (*a*) and (*b*) Morcoset AC/CS101, (*c*) and (*d*) Alfrax 17A/CS101.

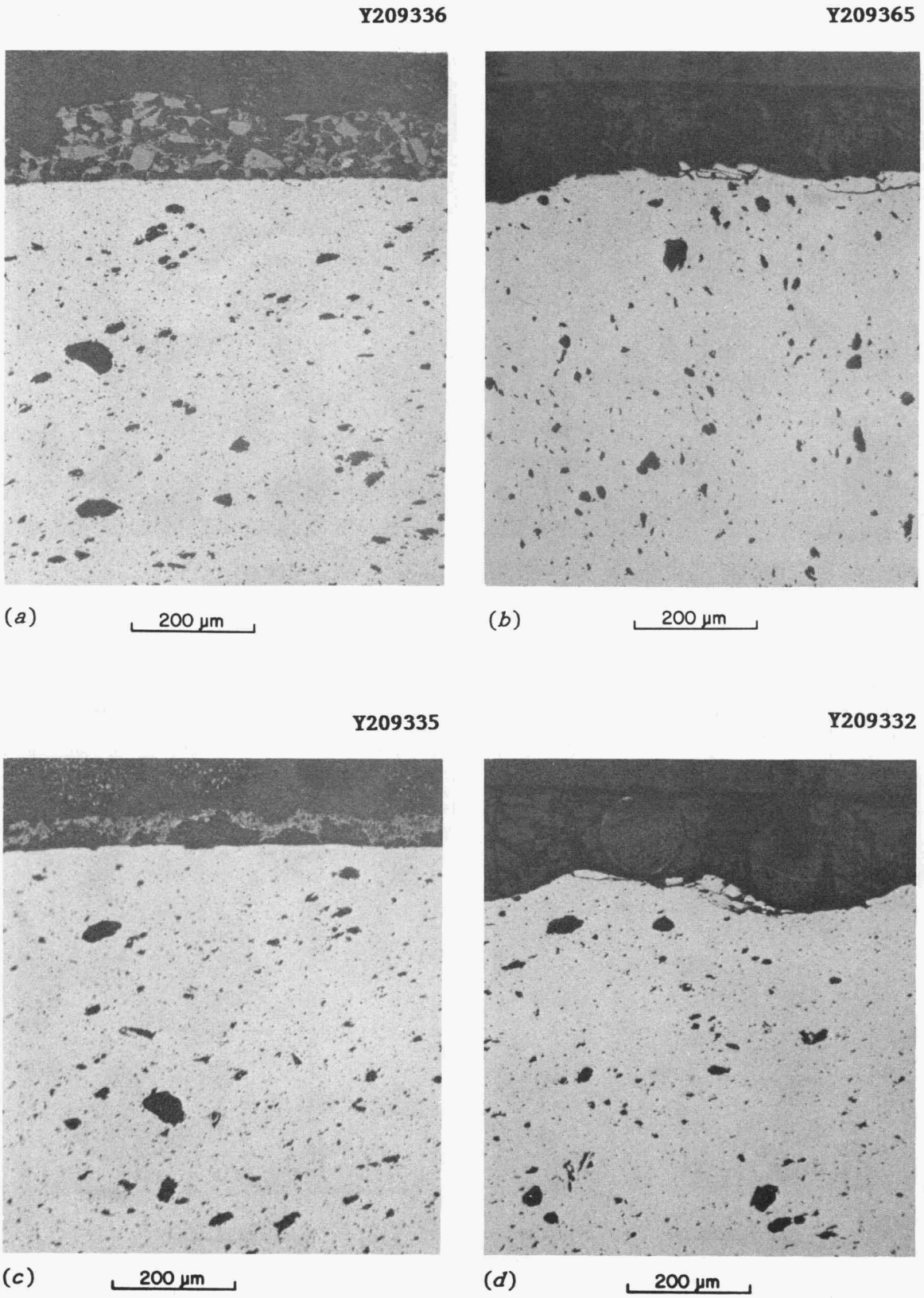

Fig. 19. Microstructures of C-90S/SA and C-ZS/SA before and after corrosion test. (*a*) and (*b*) C-90S/SA, (*c*) and (*d*) C-ZS/SA.

bonding. The SA substrates were so smooth that significant mechanical bonding did not occur. Several coatings adhered better to CS101 substrates, which were rougher because of porosity. In addition, only limited chemical bonding evidently occurred. Reactions between the principal oxide constituents of the coatings and SiC are not thermodynamically favored; however, the oxides could react with the thin SiO_2 film on the SiC to form solutions and/or compounds. Adherence would then be critically dependent on the coefficients of thermal expansion of the substrate, reaction layer, and any unreacted coating. The mass of the SiO_2 film, which is estimated to be only ~1 μm thick, might have been too small to produce an effective transition layer.

The coatings were applied by dipping, roll dipping, or air spraying at room temperature. At this stage, the coatings consisted of loosely bound particles. The first heating, usually to 1200°C, caused some sintering or reaction among the particles, resulting in a stronger, denser material. Table 2 shows that the coatings had, or probably had, higher coefficients of thermal expansion than the SiC substrates. Thus, the coatings shrank more during the first cooling than the substrates, causing the cracking and spalling frequently observed. Subsequent heating and cooling cycles caused additional damage by the same mechanism.

Coating adherence was also a critical concern in another coating study,[18] in which Y_2O_3-stabilized ZrO_2 coatings were applied to reaction-bonded Si_3N_4, sintered Si_3N_4, and sintered SiC. The SiC material was Hexoloy SA, the same material designated SA-1 and SA-2 in the current study. The ZrO_2 coating was applied by electron beam–physical vapor deposition. Various surface treatments were used to improve adherence of coatings: lapping; interlayers applied by sputtering, chemical vapor deposition, and sol-gel techniques; oxidation in air; and roughening by laser texturing. The results showed clearly that adherence was improved by surface roughness: either natural roughness due to porosity or that created by laser texturing. Oxidation in air caused deterioration of adherence, apparently because of the formation of zirconium silicate ($ZrSiO_4$) at the interface. Sputtered metallic layers oxidized and caused loss of adherence. A sol-gel Al_2O_3 interlayer aided adherence of the

ZrO_2 coating to SiC substrates, but coating adherence degraded during thermal-cycle tests to 1375°C. Laser texturing was most beneficial to adherence of ZrO_2 coatings to SiC; however, some decrease in strength occurred because of surface defects associated with the technique. These results,[18] and those obtained in the current study show that adherence of ceramic coatings to SiC is not easily attained.

Although most of the results of the current study were not encouraging, some indications of potential success were revealed:

- Coatings adhered better to CS101 substrates than to relatively smoother SA substrates.
- Coatings based on Al_2O_3 and ZrO_2 survived 50 or more thermal cycles between 200 and 1200°C.
- Coated specimens exhibited less corrosion than an uncoated specimen in a very severe corrosion test.

These results suggest that the benefit of coatings to SiC substrates during a corrosion process could be improved by higher density and greater thickness of the coatings. In the current study, the corrosion-tested coatings were quite porous and only 0.1 to 0.2 mm thick. Denser and thicker coatings might be more resistant to penetration by corrosion atmospheres and would provide more material to increase the refractoriness of the reaction product. Problems with differential thermal expansion, however, might be more serious in thicker coatings.

The results that have been presented can be summarized as follows:

- Most coatings did not survive the initial thermal cycle. During heating, the loosely bonded particles of the coatings sintered or reacted to form a coherent mass; but during cooling, the larger coefficients of thermal expansion (relative to SiC) caused cracking and spalling.
- Coatings adhered better to inherently rougher CS101 substrates than to relatively smooth SA substrates. Penetration of the coatings into surface pores caused better adherence.

- Specimens coated with Al_2O_3- and ZrO_2-based materials corroded less than an uncoated specimen. The reaction products of coated specimens evidently were more refractory because of their relatively high Al_2O_3 or ZrO_2 content. These more refractory reaction products partially inhibited oxidation of the substrates.

10. ACKNOWLEDGMENTS

Thanks are extended to those who assisted in this work: P. J. Jones for the preparation of coating, heat treatments, and corrosion testing; J. R. Mayotte for the ceramographic examination; D. P. Stinton and E. L. Long, Jr. for the technical review of the manuscript; A. J. Moorhead for technical discussions and helpful suggestions; F. W. Christie and B. B. Hickey for preparation of the draft; and M. R. Upton for final preparation of the report.

11. REFERENCES

1. P. W. Ward, "Ceramic Tube Heat Recuperator–A User's Experience," pp. 31–41 in *Advances in Ceramics, Vol. 14, Ceramics in Heat Exchangers*, ed. B. D. Foster and J. B. Patton, The American Ceramic Society, Columbus, Ohio, 1985.

2. R. G. Graham, "Development of an Air-to-Air Heat Exchanger with All-Ceramic Internals," pp. 43–48 in *Advances in Ceramics, Vol. 14, Ceramics in Heat Exchangers*, ed. B. D. Foster and J. B. Patton, The American Ceramic Society, Columbus, Ohio, 1985.

3. M. Coombs, D. Kotchick, and H. Strumpf, "A High-Temperature Ceramic Recuperator for Industrial Applications," pp. 49–50 in *Advances in Ceramics, Vol. 14, Ceramics in Heat Exchangers*, ed. B. D. Foster and J. B. Patton, The American Ceramic Society, Columbus, Ohio, 1985.

4. J. E. Snyder and D. R. Petrak, "Design and Materials Selection for a High-Temperature Burner-Duct Recuperator," pp. 59–77 in *Advances in Ceramics, Vol. 14, Ceramics in Heat Exchangers*, ed. B. D. Foster and J. B. Patton, The American Ceramic Society, Columbus, Ohio, 1985.

5. K. O. Smith, T. E. Easler, and R. B. Poeppel, "Experimental Assessment of an Axially Finned Ceramic Tube Heat Exchanger," pp. 79–96 in *Advances in Ceramics, Vol. 14, Ceramics in Heat Exchangers*, ed. B. D. Foster and J. B. Patton, The American Ceramic Society, Columbus, Ohio, 1985.

6. R. G. Graham, "Vertical Tube-Style, All-Ceramic, Air-to-Air Heat Exchanger," pp. 97–101 in *Advances in Ceramics, Vol. 14, Ceramics in Heat Exchangers*, ed. B. D. Foster and J. B. Patton, The American Ceramic Society, Columbus, Ohio, 1985.

7. M. Coombs, H. Strumpf, and D. Kotchick, "A Ceramic Finned-Plate Recuperator for Industrial Applications," pp. 127–37 in *Advances in Ceramics, Vol. 14, Ceramics in Heat Exchangers*, ed. B. D. Foster and J. B. Patton, The American Ceramic Society, Columbus, Ohio, 1985.

8. A. D. Russell, C. E. Smeltzer, and M. E. Ward, *Waste Heat Recuperation for Aluminum Furnaces*, GRI-81/0160, Solar Turbines, Inc., San Diego, Calif., April 1983.

9. J. I. Federer et al., *Analysis of Candidate Silicon Carbide Recuperator Materials Exposed to Industrial Furnace Environments*, ORNL/TM-9677, July 1985.

10. J. I. Federer and P. J. Jones, *Oxidation/Corrosion of Metallic and Ceramic Materials in an Aluminum Remelt Furnace*, ORNL/TM-9741, December 1985.

11. G. W. Weber and V. J. Tennery, *Materials Analyses of Ceramics for Glass Furnace Recuperators*, ORNL/TM-6970, November 1979.

12. N. S. Jacobson and J. L. Smialek, "Hot Corrosion of Sintered α-SiC at 1000°C," *J. Am. Ceram. Soc.* **68**(8), 432–39 (August 1985).

13. J. I. Federer et al., *Corrosion of SiC Ceramics in Synthetic Combustion Atmospheres Containing Halides*, ORNL-6258, December 1985.

14. N. S. Jacobson, "Kinetics and Mechanism of Corrosion of SiC by Molten Salts," *J. Am. Ceram. Soc.* **69**(1), 74–82 (January 1986).

15. N. S. Jacobson, C. A. Stearns, and J. L. Smialek, "Burner Rig Corrosion of SiC at 1000°C," *Adv. Ceram. Mater.* **1**(2), 154–61 (April 1986).

16. J. I. Federer, "Corrosion of SiC Ceramics by Na_2SO_4," *Adv. Ceram. Mat.* **3**(1), 56–61 (January 1988).

17. J. I. Federer and A. J. Moorhead, *Compilation of Information on Commercially Available Ceramic Coatings for High-Temperature Applications*, ORNL/TM-9875, December 1985.

18. J. Schienle and J. Smyth, *High Temperature Coating Study to Reduce Contact Stress Damage of Ceramics*, ORNL/Sub/84-47992/1, March 1987.

INTERNAL DISTRIBUTION

1–2. Central Research Library
3. Document Reference Section
4–5. Laboratory Records Department
6. Laboratory Records, ORNL RC
7. ORNL Patent Section
8. R. L. Beatty
9. P. F. Becher
10. T. M. Besmann
11. R. A. Bradley
12. C. R. Brinkman
13. A. J. Caputo
14. R. S. Carlsmith
15. D. F. Craig
16. J. R. DiStefano
17–21. J. I. Federer
22. E. P. George
23. C. Hsueh
24. D. R. Johnson
25. R. R. Judkins
26. J. R. Keiser
27. H. E. Kim
28. O. F. Kimball
29. R. T. King
30. E. L. Long Jr.
31. C. J. McHargue
32. A. J. Moorhead
33. M. Olszewski
34. G. F. Pedraza
35. A. C. Schaffhauser
36. V. K. Sikka
37. D. P. Stinton
38–40. P. T. Thornton
41. D. R. Wilson
42. A. Zucker
43. H. D. Brody (Consultant)
44. G. Y. Chin (Consultant)
45. F. F. Lange (Consultant)
46. W. D. Nix (Consultant)
47. D. P. Pope (Consultant)
48. E. R. Thompson (Consultant)

EXTERNAL DISTRIBUTION

49–50. AIRESEARCH MANUFACTURING COMPANY, 2525 W. 190th Street, Torrance, CA 90509

M. G. Coombs
D. M. Kotchick

51. BABCOCK AND WILCOX, P.O. Box 239, Lynchburg, VA 24505

W. P. Parks, Jr.

52. COMBUSTION ENGINEERING, INC., 911 West Main Street, Chattanooga, TN 37402

C. H. Sump

53. CONSOLIDATED NATURAL GAS, 11001 Cedar Avenue, Cleveland, OH 44106

J. Bjerklie

54–56. COORS PORCELAIN COMPANY, 600 Ninth Street, Golden, CO 80501

C. Dobbs
R. Kleiner
D. Roy

57–58. GTE PRODUCTS CORPORATION, Hawes Street, Towanda, PA 18848

J. L. Ferri
J. Gonzalez

59. HAGUE INTERNATIONAL, 3 Adam Street, South Portland, MA 04106

S. B. Young

60–61. IDAHO NATIONAL ENGINEERING LABORATORY, P.O. Box 1625, Idaho Falls, ID 83415

F. W. Childs
M. S. Sohal

62–63. IIT RESEARCH INSTITUTE, 10 West 35th Street, Chicago, IL 60616

J. W. Adams
D. C. Larsen

64–65. NORTON COMPANY, Worcester, MA 01606

B. D. Foster
M. L. Torti

66. PENNSYLVANIA STATE UNIVERSITY, 201 Steidle Building, University Park, PA 16801

R. E. Tressler

67–68. SOLAR TURBINES INCORPORATED, P.O. Box 8537, San Diego, CA 92138-5376

M. E. Ward
M. Van Roode

69. STANDARD OIL ENGINEERED MATERIALS COMPANY, Structural Ceramics Division, P.O. Box 10549, Niagara Falls, NY 14302

S. Halstead

70–72. TECOGEN, INC., P.O. Box 9046, Waltham, MA 02254-9046

W. E. Cole
K. D. Patch
S. Ronald Wysk

73. UNIVERSITY OF ILLINOIS AT CHICAGO, P.O. Box 4348, Chicago, IL 60680

M. J. McNallan

74. DOE, IDAHO OPERATIONS OFFICE, 550 Second Street, Idaho Falls, ID 83401

G. R. Peterson

75. DOE, MORGANTOWN ENERGY TECHNOLOGY CENTER, P.O. Box 880, Morgantown, WV 26505

J. M. Hobday

76. DOE, OAK RIDGE OPERATIONS OFFICE, P.O. Box E, Oak Ridge, TN 37831

Office of Assistant Manager for Energy Research and Development

77–93. DOE, OFFICE OF INDUSTRIAL CONSERVATION, 1000 Independence Ave., Forrestal Building, Washington, DC 20585

J. Eustis
S. L. Richlen
J. R. Rossmeissl (15)

94–103. Office of Scientific and Technical Information, Office of Information Services, P. O. Box 62, Oak Ridge, TN 37831

For distribution by microfiche as shown in DOE/TIC-4500, Distribution Category UC-95 (Energy Conservation).

☆U.S. GOVERNMENT PRINTING OFFICE 1988–548-118/60177